GGI_TLM Integrated Multi-conductor cable model

George Green Institute of Electromagnetics Research

School of Electrical and Electronic Engineering,

University of Nottingham

Contents

1 Introduction

This document describes the techniques developed at the University of Nottingham for embedding cable models into the GGI_TLM code. The embedded cable model is designed to be self consistent in that it takes proper account of both coupling from external fields onto cables and also radiation from cables. The method is capable of modeling Multi-conductor cables, including shielded cables with frequency dependent transfer impedance models. Voltage sources and frequency dependent loads may be incorporated at cable terminations.

The report firstly describes the mesh generation process which builds the cable model which must be solved in GGI_TLM. The basic theory implementing the self consistent cable model is derived in detail for a single wire model, this model is then generalized firstly to model multi-conductor cables and subsequently to model shielded cables. The solution of the coupled TLM field/ cable model is derived in the most general case of a multi-conductor cable junction with shielded cables at a cell centre and for a multi-conductor cable termination at a cell face with sources, loads and boundary conditions for connector to conducting surfaces applied. The implementation of frequency dependent impedances within the model is described. This model which is based on digital filter techniques allows the modeling of lumped impedances or modeling frequency dependent transfer impedance of shielded cables.

Within **GGI_TLM** cables are defined to be systems of conductors which run through the problem space without changing their cross section configuration along their length. A cable may have one conductor such as a simple cylindrical wire, or multiple conductors such as a ribbon cable or coaxial cable. Cables may include shielded conductors. Cables must be terminated at both ends to a defined junction.

A junction may be situated at a cell centre or on the surface of a mesh cell. Boundary conditions may be applied on surface junctions which allows conductors to be electrically connected to surfaces as well as being connected amongst themselves. A junction at a surface allows cables to be connected from either side of the cell surface thus for example a coaxial cable may have its shield terminated to a ground plane while the inner conductor is allowed to pass through. In this way coaxial feeds trough ground planes can be modeled.

At a cell centre junction, conductors from the six faces belonging to the cell may be connected in an arbitrary manner so that complex networks can be formed.

Lumped loads and sources may be placed at the ends of cables.

Bundles are formed when more than one cable runs along the same path through the mesh.

2 Mesh Generation for cables

Cables are defined with a particular cross section which may include multiple cores and screens so each cable may be a multi-conductor. A cable route through the problem space is defined as a

sequence of lines. The lines must be continuous. A junction must be specified at each end of the cable, this may take the form of an open circuit condition as in the ends of a dipole, a termination to a surface via a lumped load and source or a connection to another cable at the junction, again incorporating lumped elements and sources.

Complex wiring within a model is specified in a three stage manner. Firstly a number of lines are specified with the problem space in the input file (figure 2.1.) These lines are then put onto the structured mesh automatically by **GGI_TLM**. Meshed lines run between cell centres on the mesh. It should be noted that lines which run through the same cell in the structured mesh will be snapped together.

The cable mesh follows the line mesh with the addition of the junction points which may be situated at a cell centre or on a cell face (figure 2.2.)

Nodes are formed at cell centres and at points where lines intersect cell faces. Where lines meet at a cell centre a junction is formed.

The meshed cable structure defines a 1D mesh consisting of nodes connected by segments. The mesh will contain the junctions defined in the input file and also junctions formed by the meshing process as a result of changes in composition of the cable bundles formed by snapping together of the individual cables.

The cables running along each line segment in the mesh are combined to form bundles of cables (figure 2.4.) The cable bundles on the 1D cable bundle mesh are the basis for the computation.

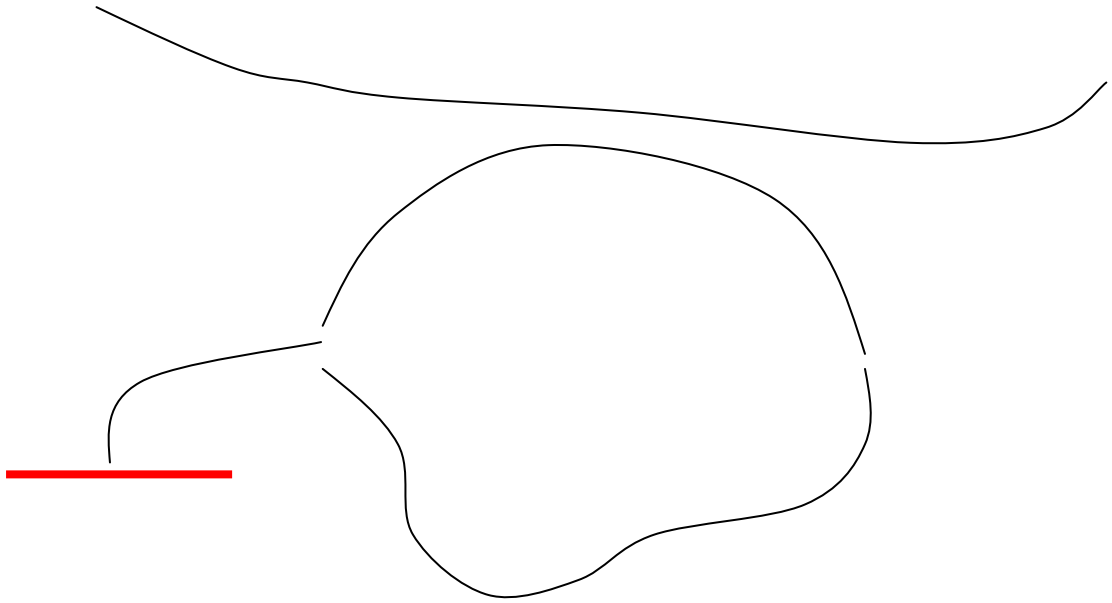

Figure 2.1. Initial line geometry

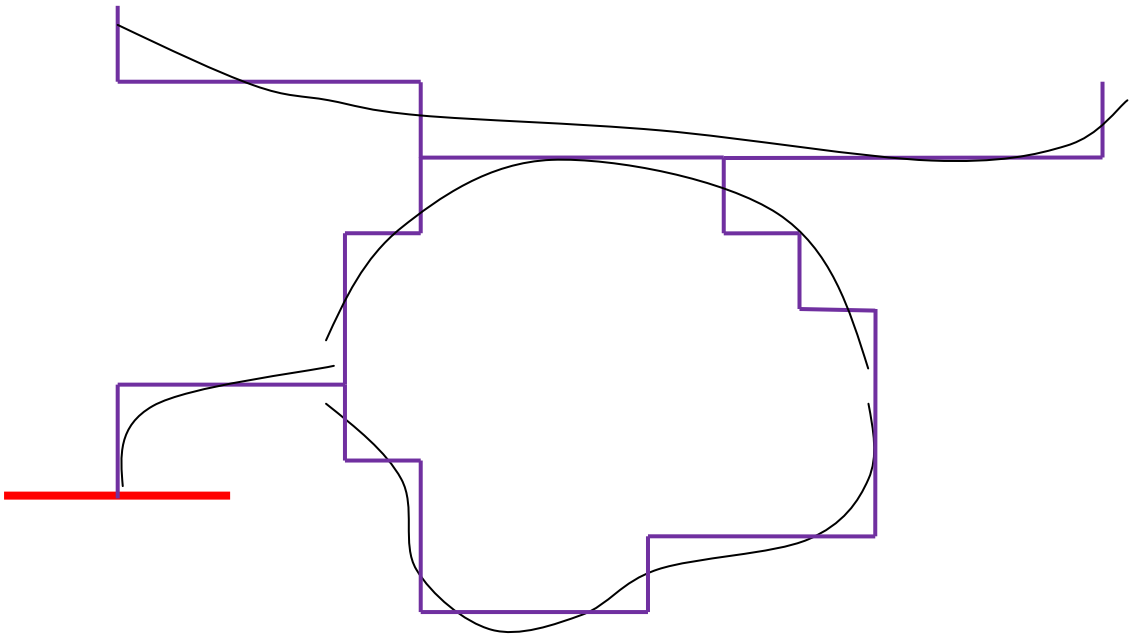

Figure 2.2.Create structured line geometry forming wire routes

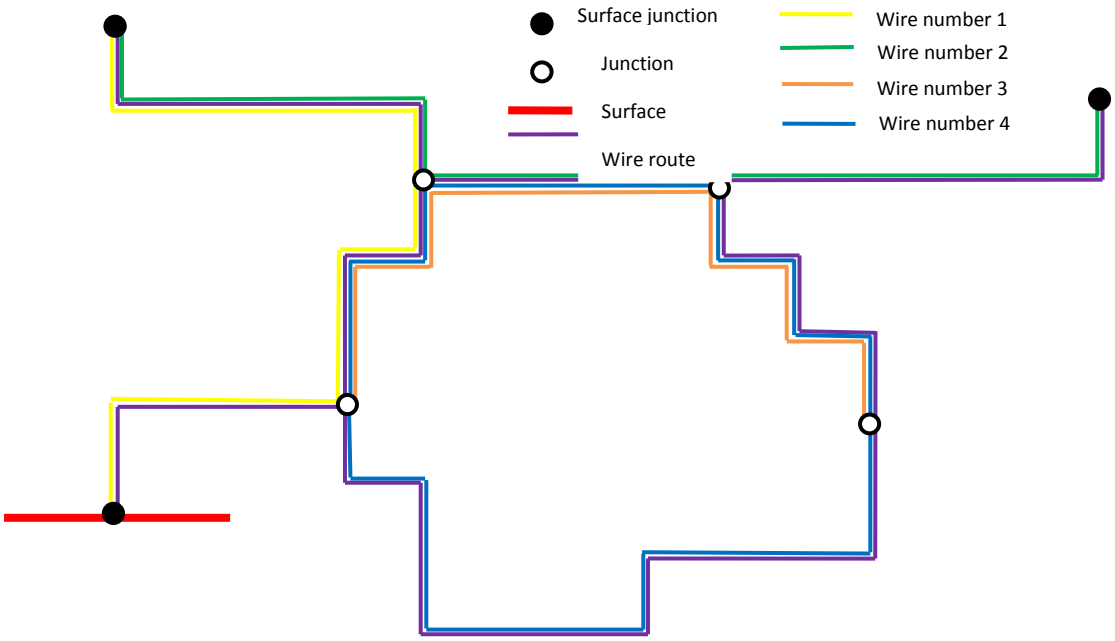

Figure 2.3. Cables follow the wire routes forming bundles.

Individual cables are assembled into bundles and the bundle parameters are calculated in the EM solver code.

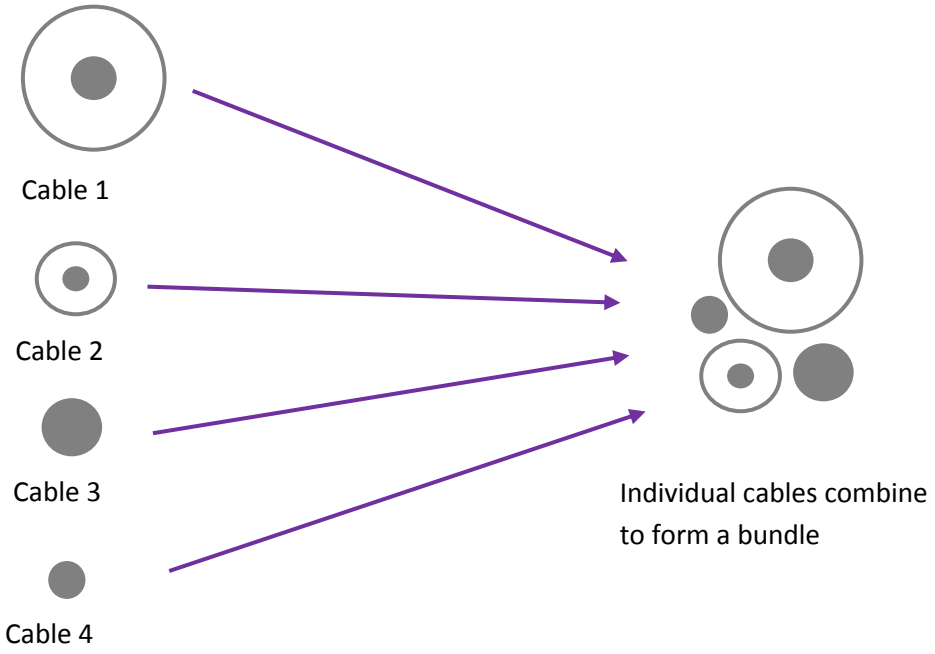

Figure 2.4. Individual cables are combined to form bundles.

Figure 2.5 shows an example of a GGI_TLM mesh including a number of cables.

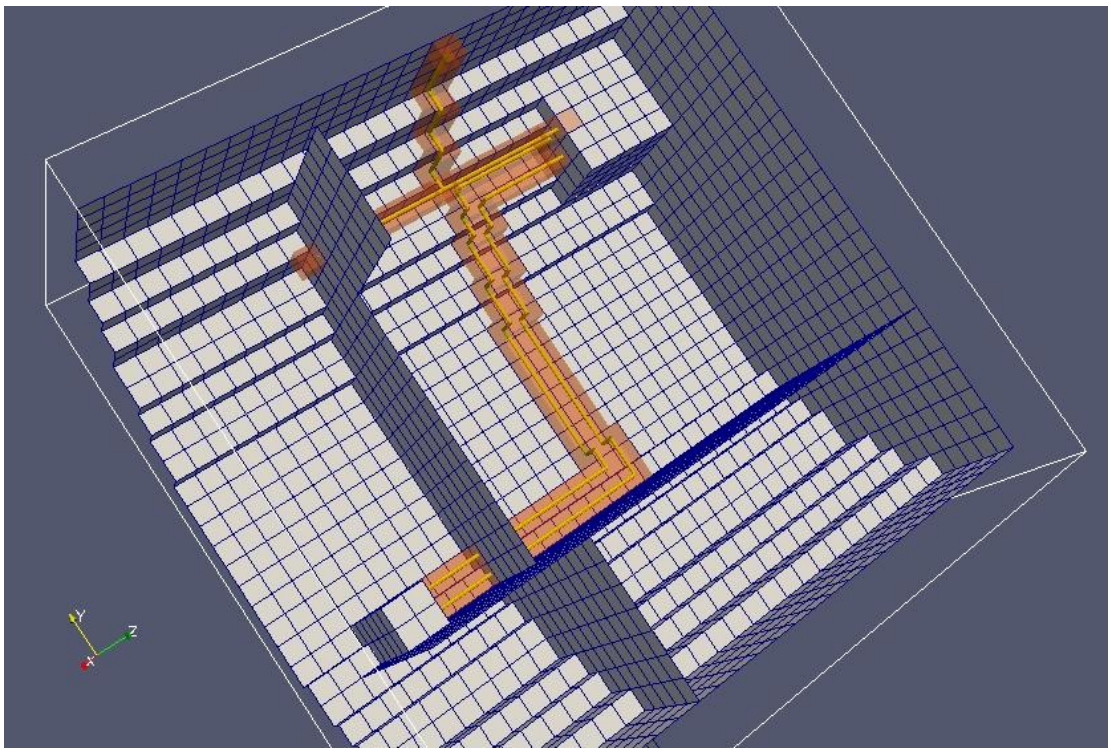

Figure 2.5. Example meshed cable model

3 The GGI_TLM self consistent cable model

3.1 TLM single wire model

The TLM cable model derivation follows that in reference [1].

The field within the volume of the TLM cell is the sum of the TLM field and the wire field as seen in figure 3.1.1.

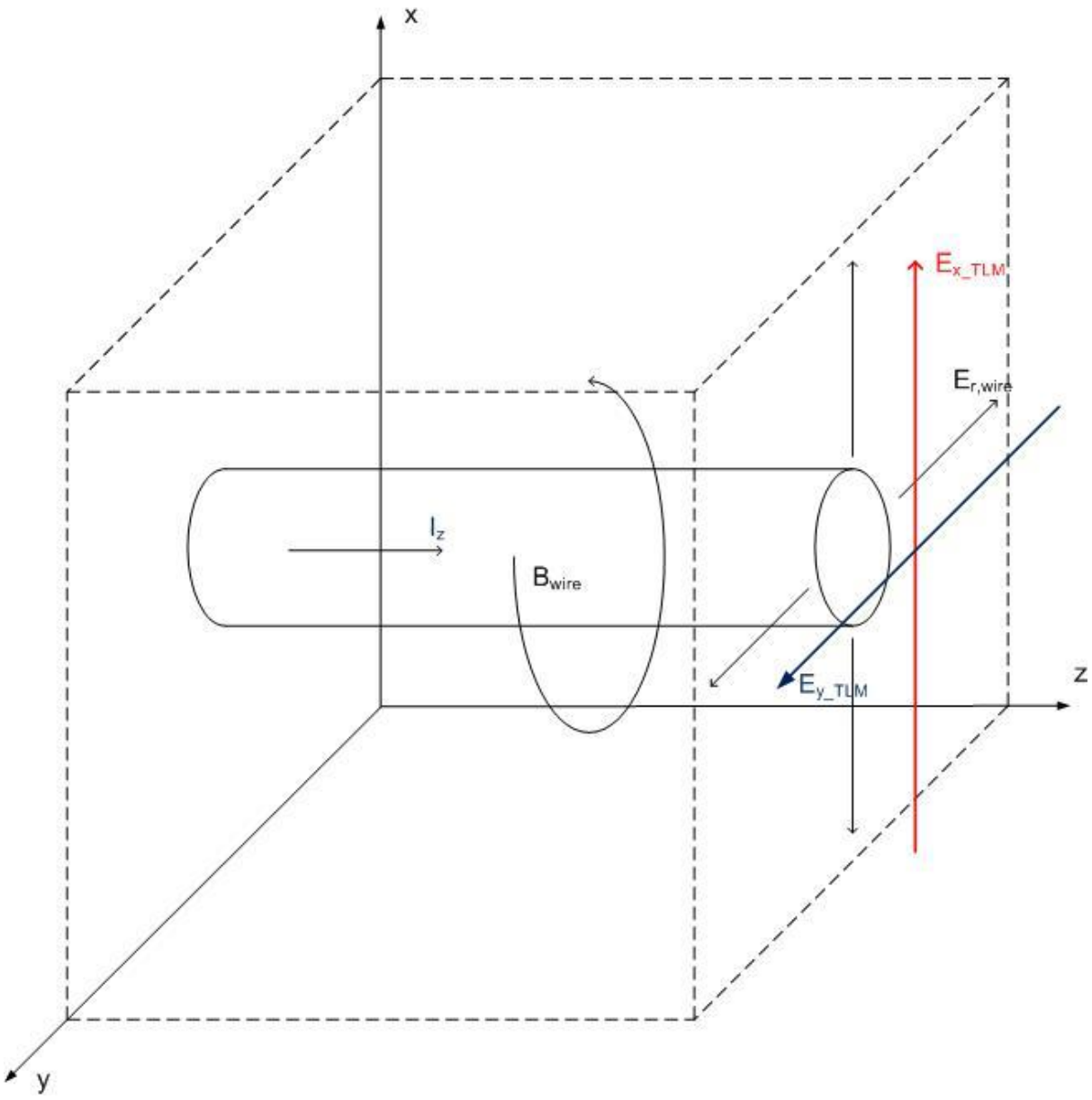

Figure 3.1.1.

The first transmission line equation is derived from Faraday's law

$$\oint_C E.dl = -\frac{\partial}{\partial t}\iint_S B.ds \qquad (3.1.1)$$

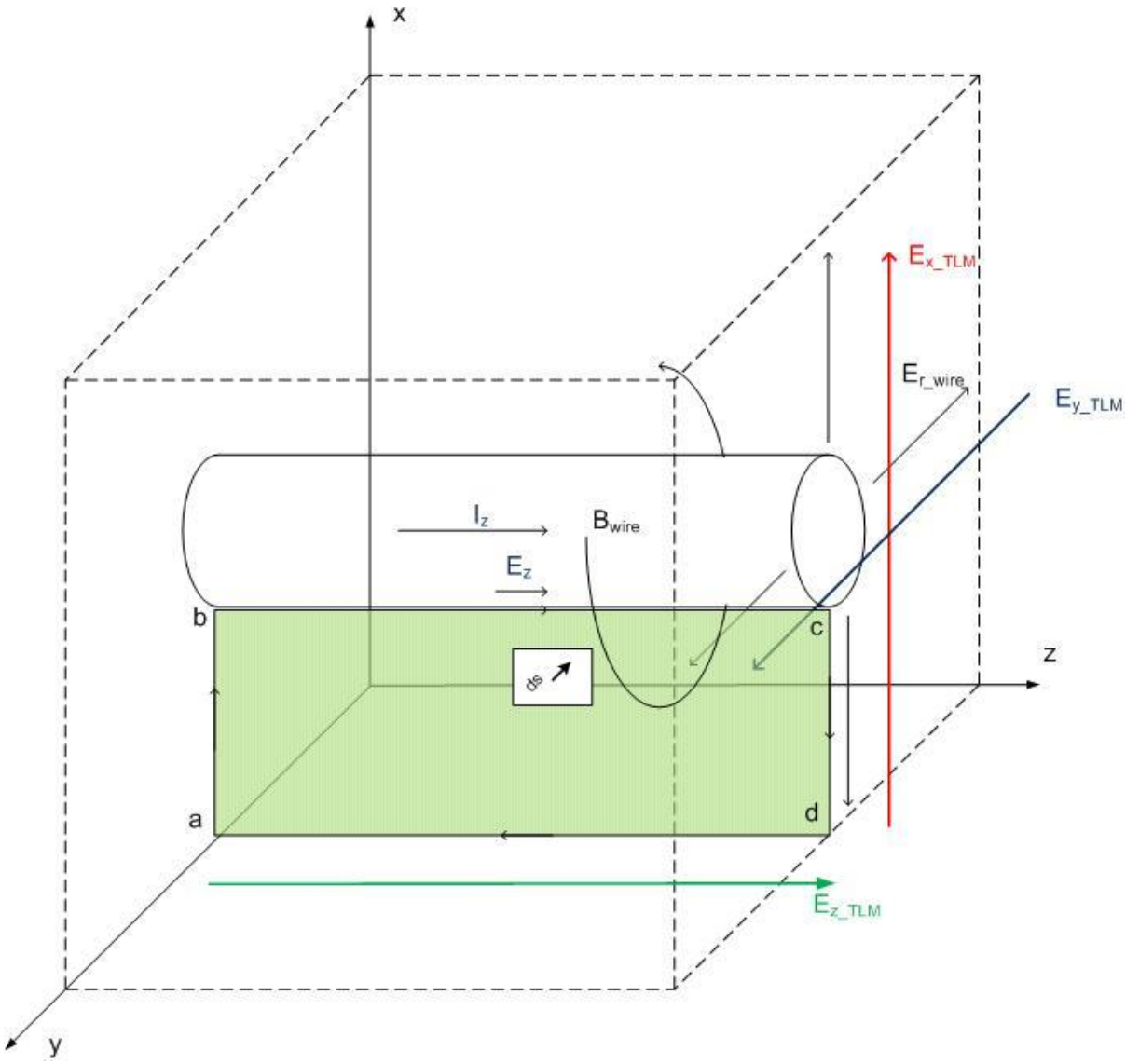

Figure 3.1.2.

Evaluating the integrals on the surface enclosed by the contour along the centre line of the TLM cell face, to the surface of the conductor at the cell centre, along the conductor and back out to the cell face to close the contour gives:

$$\int_a^b E_r.dl + \int_b^c E_z.dl + \int_c^d E_r.dl + \int_d^a E_z.dl = -\frac{\partial}{\partial t}\left\{\iint_S B_\phi.ds\right\} \qquad (3.1.2)$$

The magnetic field, B_ϕ, originates from the current, i_z, flowing on the wire and is related to it by the inductance hence the right hand side of equation 3.1.2 can be expressed as

$$-\frac{\partial}{\partial t}\left\{\iint_S B_\phi.ds\right\} = -L_0 \Delta z \frac{\partial I_z}{\partial t} \qquad (3.1.3)$$

The radial component of the electric field, E_r, is a result of charges on the wire. The individual integrals on the left hand side of equation 3.1.2 are evaluated as follows:

$$\int_a^b E_x.dl = \int_a^b \left(-E_{r\_wire}\left(z,t\right)+E_{x\_TLM}\left(z,t\right)\right)dl = -V\left(z,t\right)-\frac{E_{x\_TLM}\left(z,t\right)\Delta l}{2} \qquad (3.1.4)$$

The contribution from the integral along the conductor is a result of the resistive voltage loss along the cable

$$\int_b^c E_z.dl = R_0\Delta z I_z(z,t) \quad (3.1.5)$$

$$\int_c^d E_x.dl = \int_c^d \left(E_{r\_wire}\left(z+\Delta z,t\right)-E_{x\_TLM}\left(z+\Delta z,t\right)\right)dl = V\left(z+\Delta z,t\right)+\frac{E_{x\_TLM}\left(z+\Delta z,t\right)\Delta l}{2} \quad (3.1.6)$$

The electric field on the TLM cell face is evaluated as the TLM E_z field thus the integral along the TLM cell face is

$$\int_d^a E_z.dl = -E_{z\_x\min\_tlm}\Delta z \qquad (3.1.7)$$

Substituting into the original expression gives

$$-V(z,t)-\frac{E_{x\_TLM}\left(z,t\right)\Delta l}{2}+R_0\Delta z i_z+V(z+\Delta z,t)+\frac{E_{x\_TLM}\left(z+\Delta z,t\right)\Delta l}{2}-E_{z\_x\min\_tlm}\Delta z=-L_0\Delta z\frac{\partial I_z}{\partial t} \quad (3.1.8)$$

A similar analysis on contours defined on the xmax face of the cell give

$$-V(z,t)+\frac{E_{x\_TLM}\left(z,t\right)\Delta l}{2}+R_0\Delta z i_z+V(z+\Delta z,t)-\frac{E_{x\_TLM}\left(z+\Delta z,t\right)\Delta l}{2}-E_{z\_x\max\_tlm}\Delta z=-L_0\Delta z\frac{\partial I_z}{\partial t} \quad (3.1.9)$$

Similarly on the ymin and ymax faces of the cell we get the equations

$$-V(z,t)-\frac{E_{y\_TLM}\left(z,t\right)\Delta l}{2}+R_0\Delta z i_z+V(z+\Delta z,t)+\frac{E_{y\_TLM}\left(z+\Delta z,t\right)\Delta l}{2}-E_{z\_y\min\_tlm}\Delta z=-L_0\Delta z\frac{\partial I_z}{\partial t} \quad (3.1.10)$$

$$-V(z,t)+\frac{E_{y\_TLM}\left(z,t\right)\Delta l}{2}+R_0\Delta z i_z+V(z+\Delta z,t)-\frac{E_{y\_TLM}\left(z+\Delta z,t\right)\Delta l}{2}-E_{z\_y\max\_tlm}\Delta z=-L_0\Delta z\frac{\partial I_z}{\partial t} \quad (3.1.11)$$

Summing these equations and dividing by 4 eliminates the E_x and E_y components leaving

$$-V(z,t)+R_0\Delta z i_z+V(z+\Delta z,t)-E_{z\_tlm}\Delta z=-L_0\Delta z\frac{\partial I_z}{\partial t} \qquad (3.1.12)$$

Dividing by Δz and letting $\Delta z \rightarrow 0$ gives the first transmission line equation

$$\frac{\partial V(z,t)}{\partial z} + R_0 I_z + L_0 \frac{\partial I_z}{\partial t} = E_{z\_tlm} \qquad (3.1.13)$$

The second transmission line equation comes from Gauss' law applied to the surface shown in figure 3.1.3

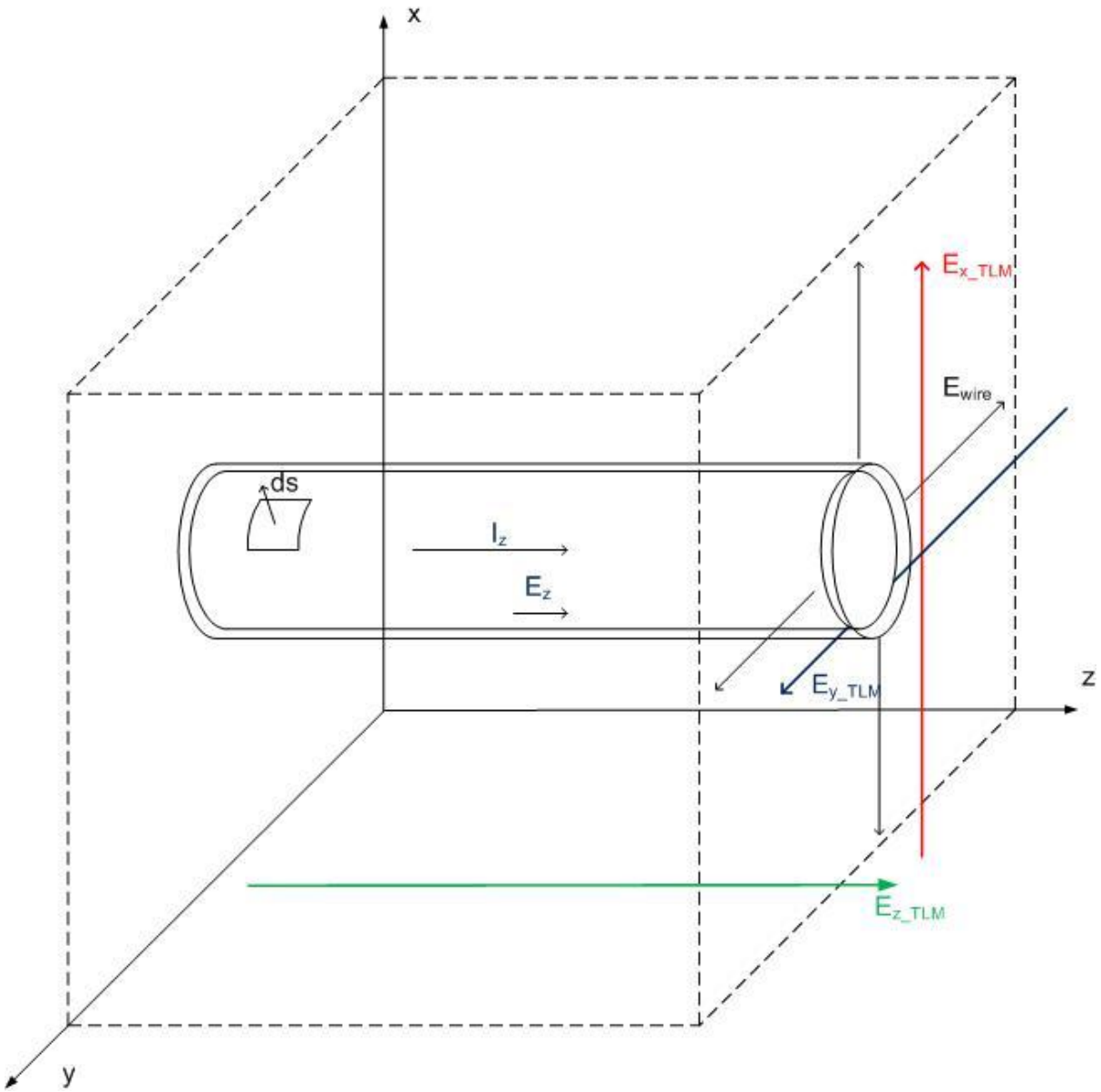

Figure 3.1.3. Gauss' law surface

$$\oiint_S J.ds = -\frac{\partial Q_{enclosed}}{\partial t} \qquad (3.1.14)$$

Over the end caps of the surface

$$\iint_{S_e} J.ds = I_z(z+\Delta z,t) - I_z(z,t) \qquad (3.1.15)$$

Across the remaining part of the surface the current density is due to the conductance of the medium in which the conductor is embedded.

$$\iint_{S_c} J.ds = G\Delta z V(z,t) \qquad (3.1.16)$$

The enclosed charge is related to the conductor voltage through the capacitance thus

$$-\frac{\partial Q_{enclosed}}{\partial t} = -C_0 \Delta z \frac{\partial V}{\partial t} \qquad (3.1.17)$$

Thus

$$I_z(z+\Delta z,t) - I_z(z,t) + G_0 \Delta z V(z,t) = -C_0 \Delta z V \qquad (3.1.18)$$

Multiplying by Δz and taking the limit as $\Delta z \rightarrow 0$ gives

$$\frac{\partial I_z(z,t)}{\partial z} + G_0 V(z,t) + C_0 \frac{\partial V(z,t)}{\partial t} = 0 \qquad (3.1.19)$$

The telegrapher's equations 3.1.13 and 3.1.19 may be modeled by a ladder network consisting of cells as shown in figure 3.1.4. When we expand the system to multi-conductors then it will be convenient to place the voltage source term in the reference conductor as seen in figure 3.1.5. If each cell represents a length Δl of transmission line connecting a TLM cell face to the cell centre then the component values may be identified as:

L	$L_0 \Delta l/2$
C	$C_0 \Delta l/2$
R	$R_0 \Delta l/2$
G	$G_0 \Delta l/2$
V_s	$E_z \Delta l/2 = -V_z/2$

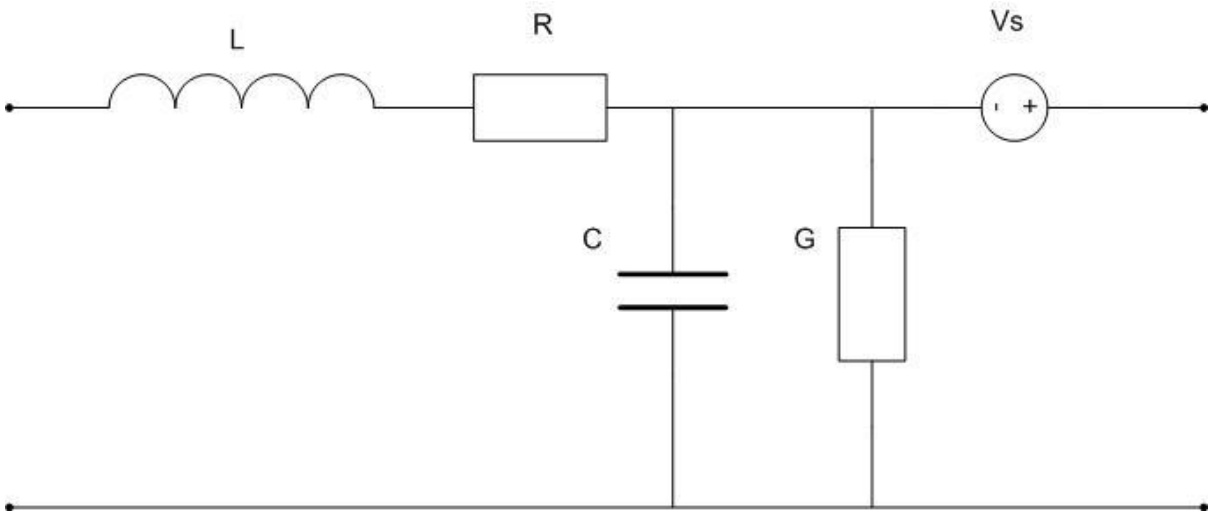

Figure 3.1.4.

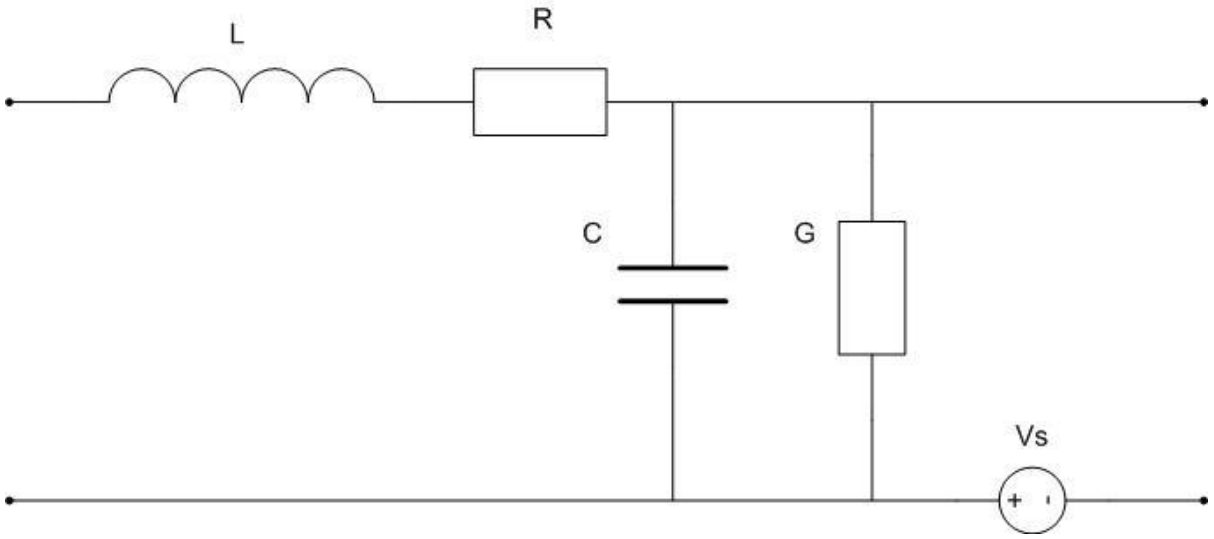

Figure 3.1.5.

A portion of the inductance and capacitance may be incorporated into a link transmission line section of impedance Z_{0w}. Any additional capacitance required may be included in an open circuit stub of impedance Z_c and additional inductance may be included in a short circuit stub of impedance Z_L thus a transmission line model of the wire propagation is derived (see figure 3.1.6.) This transmission line model is not unique, the capacitance and inductance may be distributed arbitrarily between the link line and stub lines. The distribution of the capacitance and inductance into link and stub lines will affect the dispersion characteristics of the model.

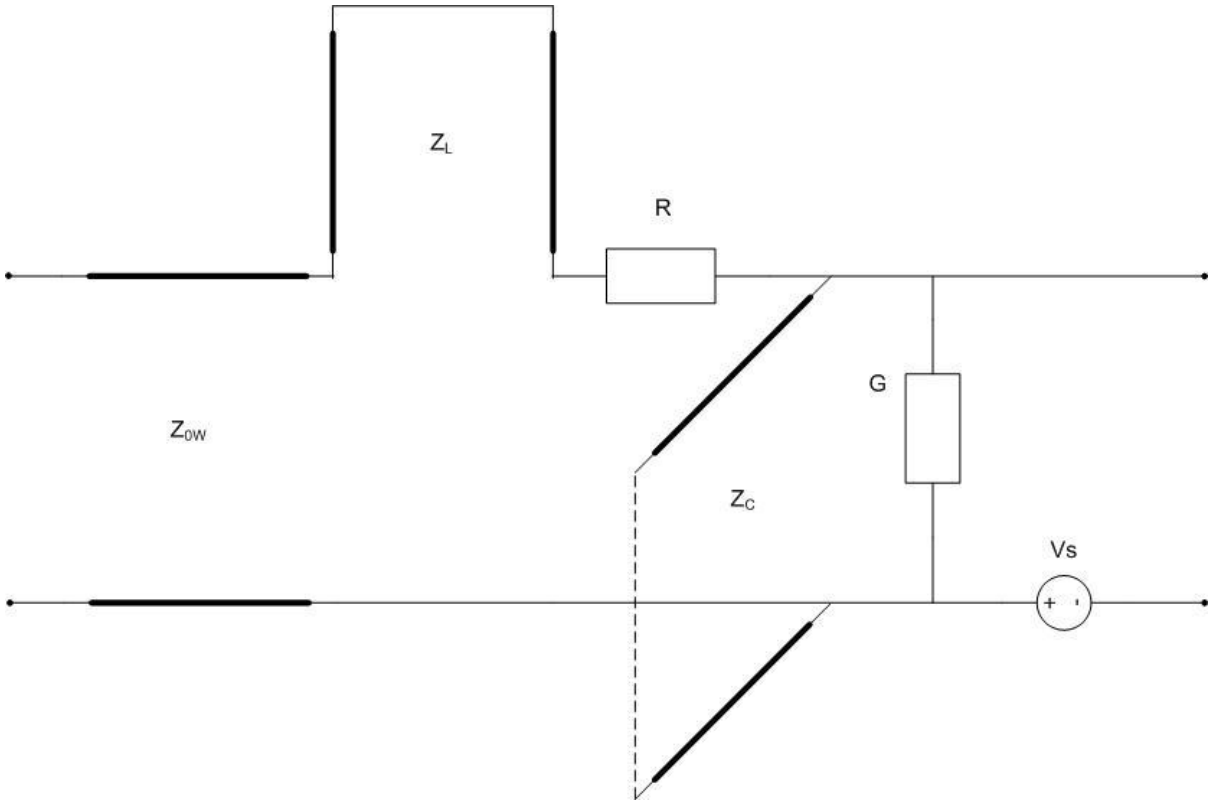

Figure 3.1.6.

A wire in the z direction is seen to link to the z component of the electric field. The z directed E field calculation in the TLM symmetrical condensed node is seen to be achieved by analysis of the shunt circuit in figure 3.1.7.

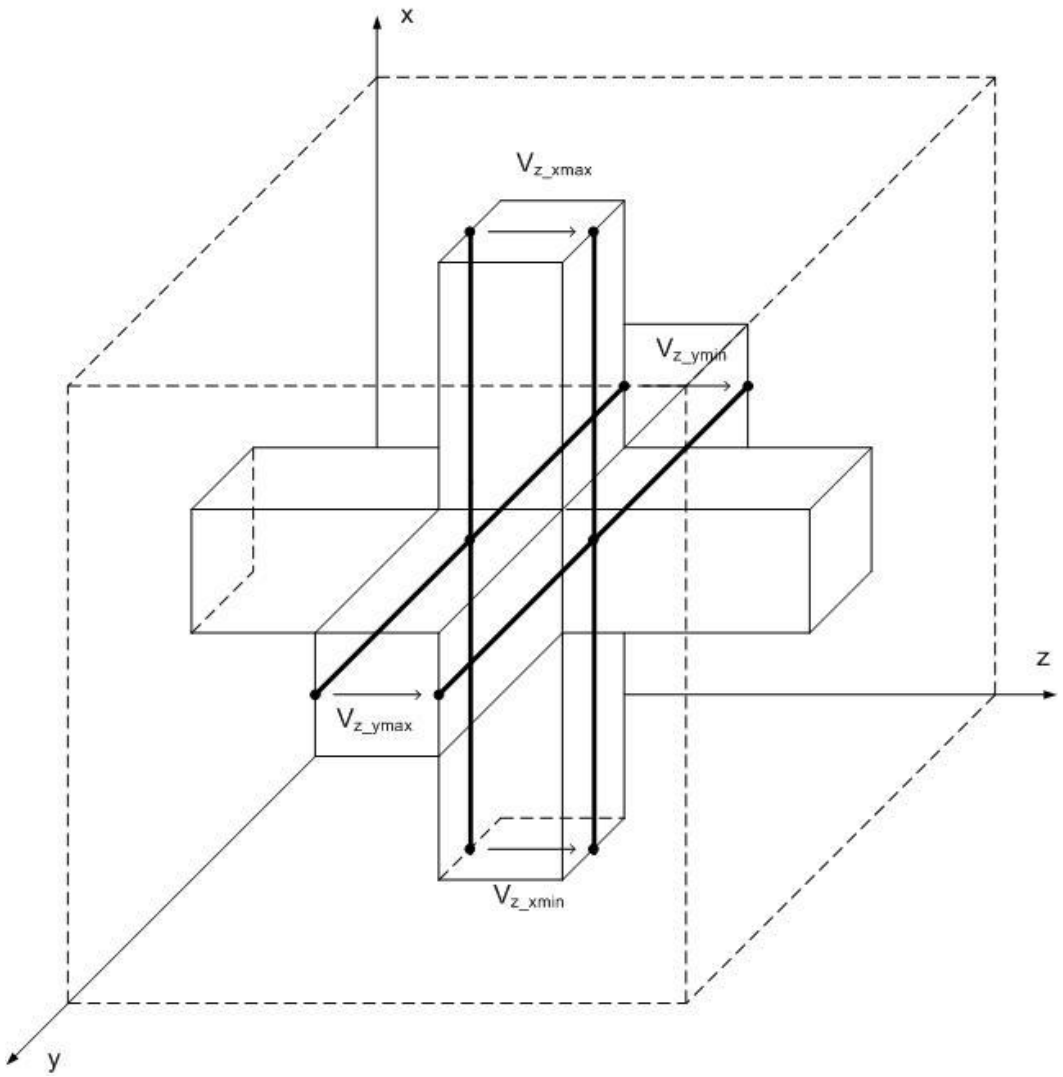

Figure 3.1.7.

The Thevenin equivalent circuit is shown in figure 3.1.8

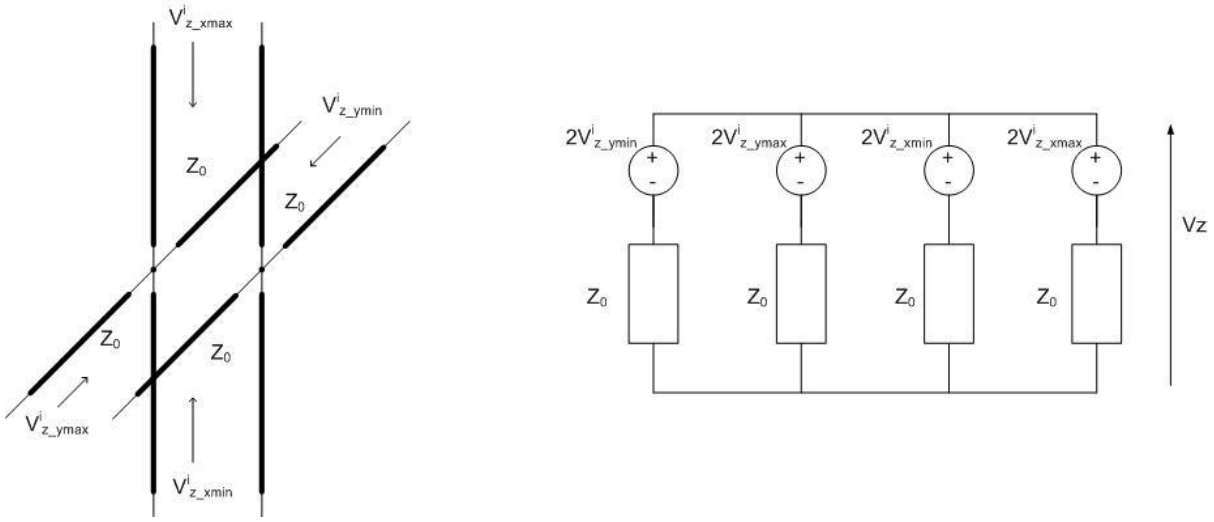

Figure 3.1.8.

The z directed current on the wire should also be taken into account in the field model so as to take proper account of the radiation from the wire. A circuit model which achieves the consistent link between TLM field model and the TLM wire model is shown in figure 3.1.9. The ideal transformer included in the circuit becomes necessary when we consider cable junctions and bends which occur at the centres of cells.

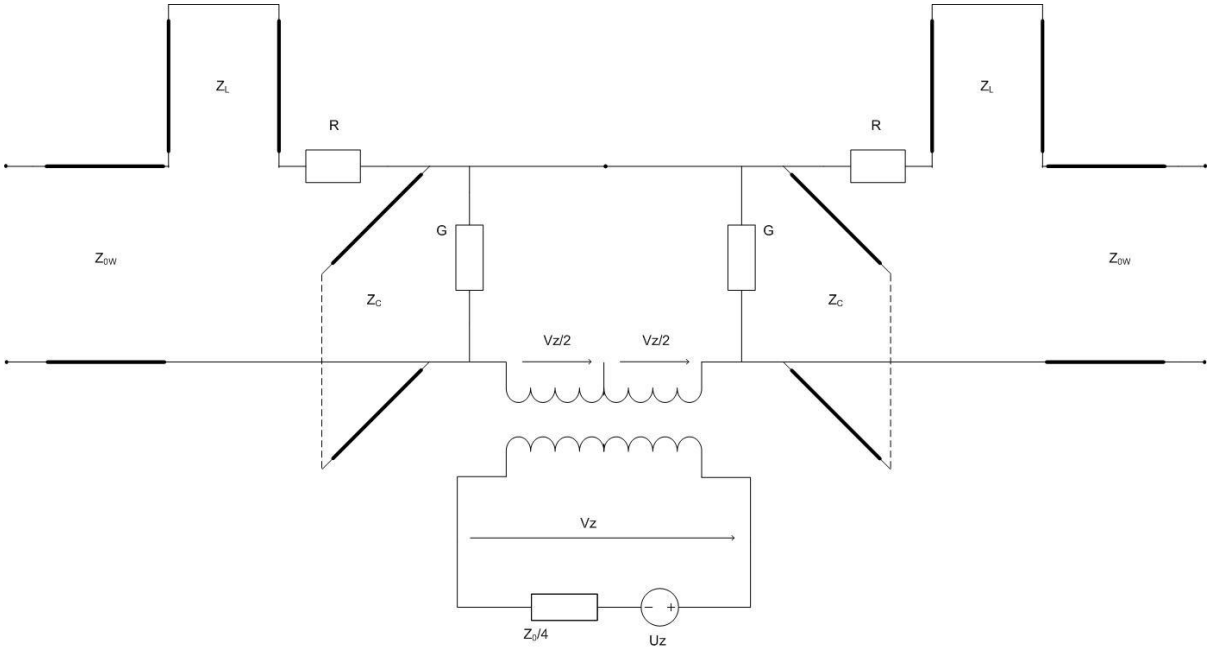

Figure 3.1.9.

It should be noted that the wire current flows through the TLM link transmission lines and therefore the wire sees the inductance of these link lines. The wire model inductance should therefore be corrected to take this additional inductance into account.

The parameters of the model may be chosen for a wire segment of length Δl/2 from cell face to cell centre as follows:

The capcacitive stub in the wire model may be eliminated if we model all the cable capacitance in the link line. The impedance of the link line is therefore given by

$$Z_{0w} = \frac{\Delta t}{2C} \qquad (3.1.20)$$

The inductance modeled by the link line is given by

$$L = Z_{0W}\frac{\Delta t}{2} \qquad (3.1.21)$$

Taking into account the inductance of the four parallel link lines $L_{link\_lines} = \frac{\Delta t Z_0}{8}$, and the fact that this inductance should be distributed over two segments of length Δl/2, the inductance of the required stub is: $L_S = L - Z_{0W}\frac{\Delta t}{2} - \frac{Z_0 \Delta t}{16}$

the impedance of the stub transmission line should be [2, 3]:

$$Z_L = \frac{2}{\Delta t}\left(L - Z_{0W}\frac{\Delta t}{2} - \frac{\Delta t Z_0}{16} \right) \qquad (3.1.22)$$

The cell centre analysis proceeds by forming a Thevenin equivalent circuit of the transmission lines, resistance and conductance elements on the left and right hand side to give the circuit in figure 3.1.10. Voltage sources and load impedances may be included in the Thevenin equivalent. Analysis of this circuit gives a solution for Vz, the TLM SCN voltage in the x direction as well as the wire current and voltage. The analysis of the equivalent circuit will be presented in a subsequent section in which the multi-conductor shielded cable model is described.

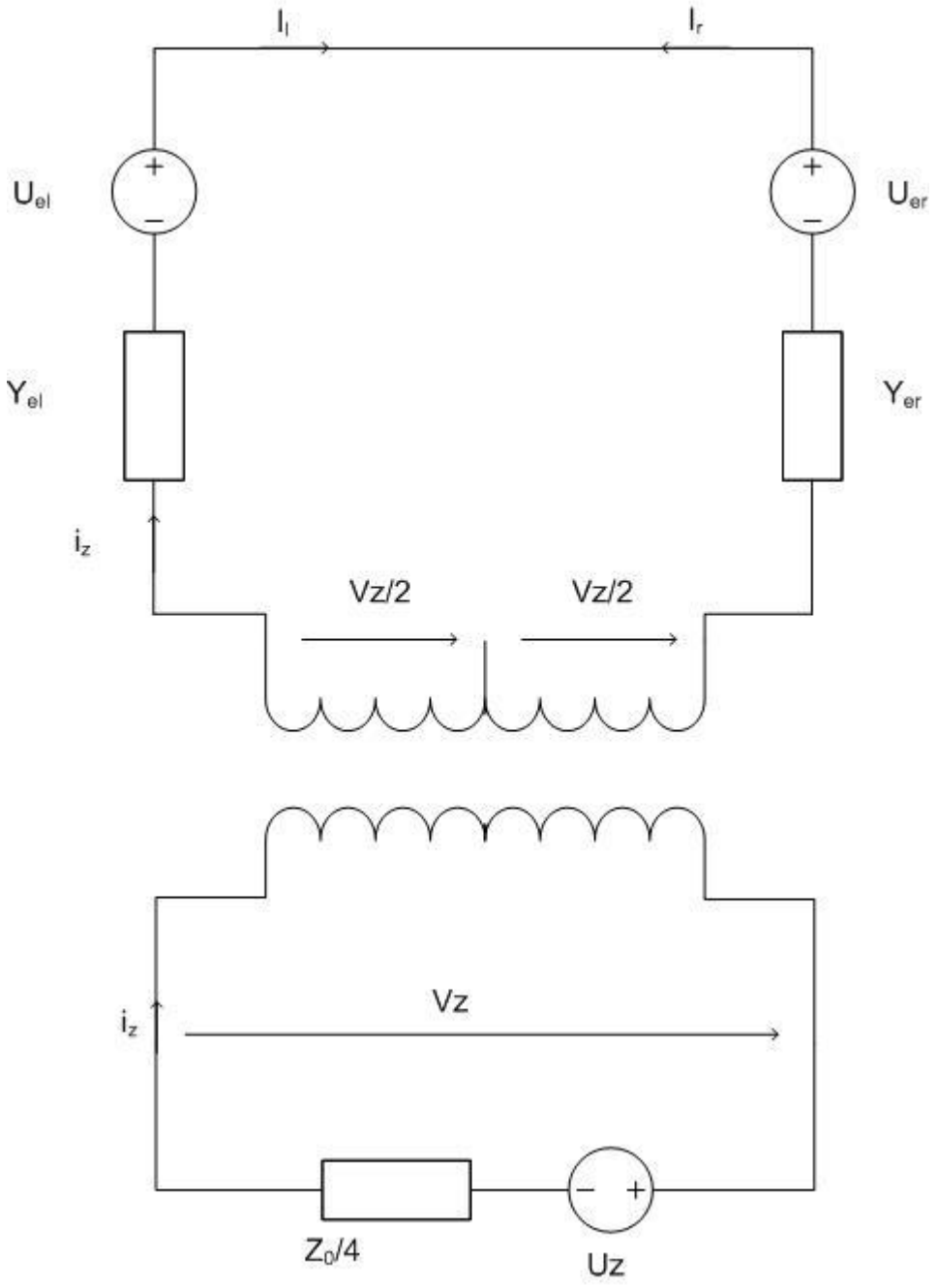

Figure 3.1.10.

The complete electrical state of the embedded wire is found at the cell centre and the appropriate voltage pulses are scattered back into the wire model link and stub lines. The voltage Vz also enables the SCN scattering calculation to proceed, taking into account the presence of the wire.

If we have continuity of wires at cell faces therefore the connection process for wire voltage pulses simply consists of a swap of voltage pulses on the wire link lines (figure 3.1.11).

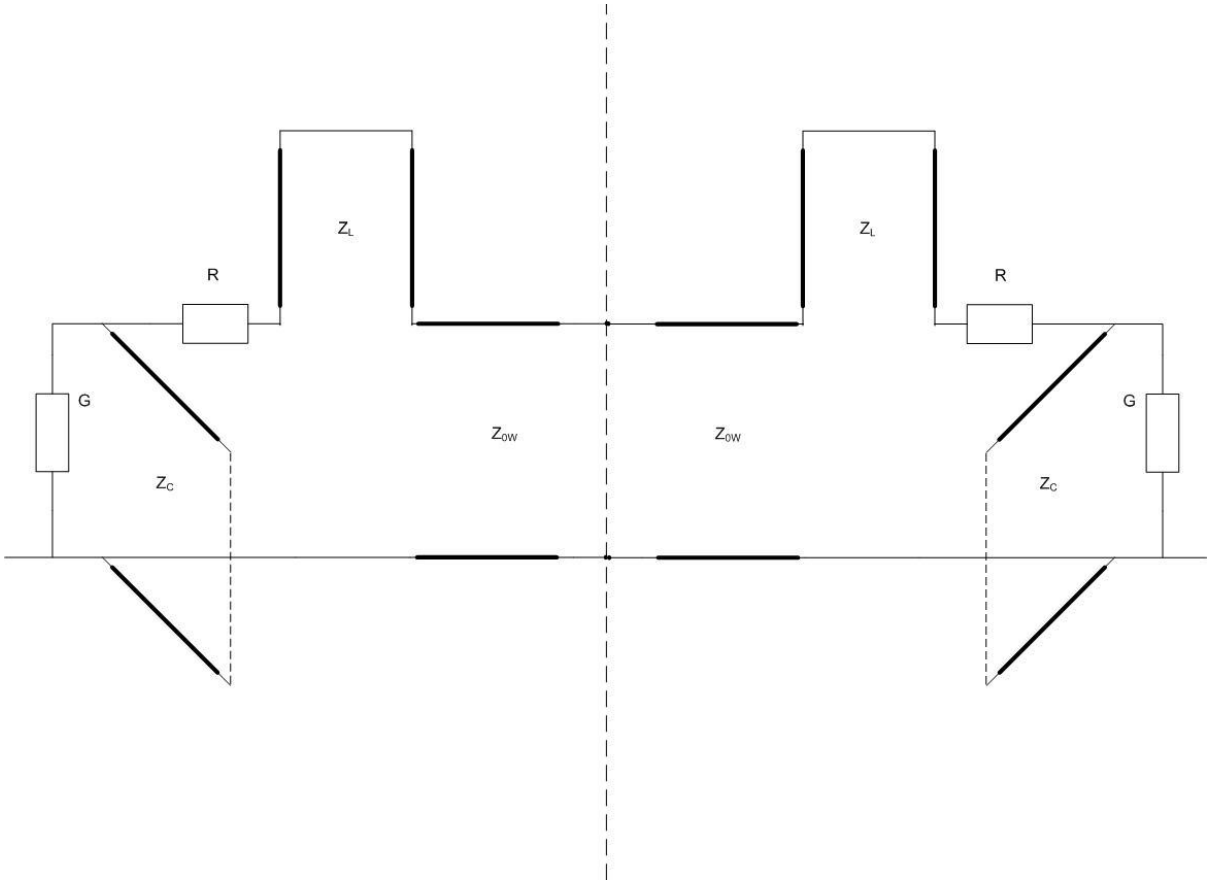

Figure 3.1.11. Cable model at a TLM cell face.

Termination to conducting surfaces may be achieved at a cell face by applying a voltage reflection coefficient of -1 (figure 3.1.12) or an open circuit by a voltage reflection coefficient of +1. More complex termination conditions may be incorporated into the model including voltage sources and frequency dependent loads using the method described in section 3.2.

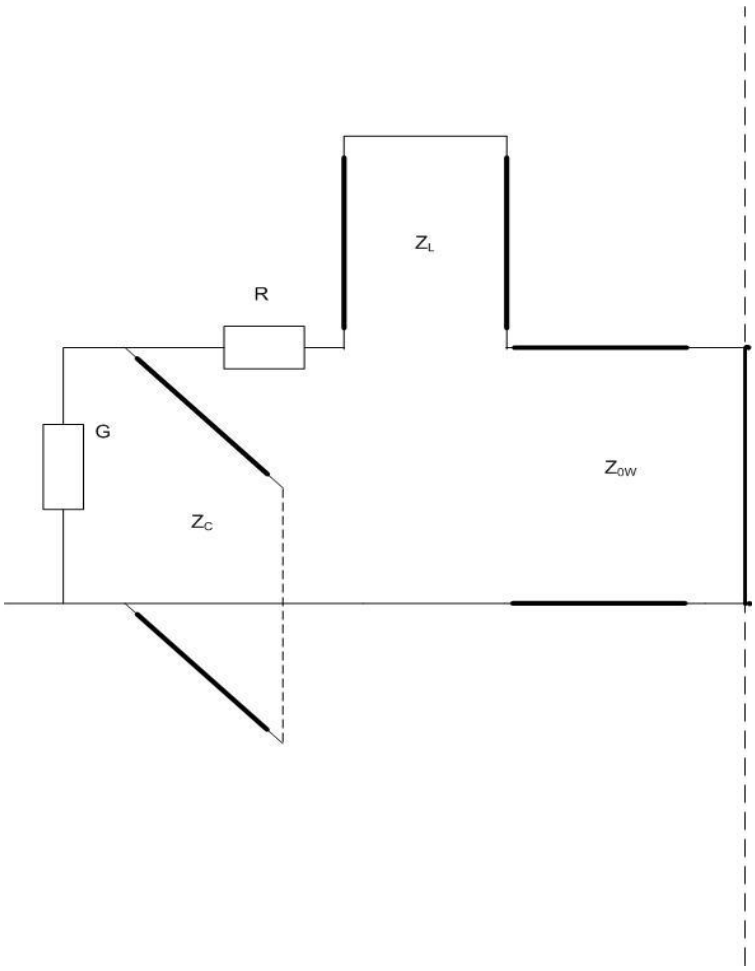

Figure 3.1.12. Cable termination at a TLM cell face.

The embedded wire model is an equivalent circuit model and is therefore stable provided that all component values are positive thus we can always establish the stability of the model.

3.2 TLM multi-conductor wire model

The single wire model described in section 3.1 is readily generalized to model multi-conductor cables. The first thing that must be done is to derive a multi-conductor propagation model. For a n conductor system the derivation follows that of the previous section where integration paths in Faraday's law (equation 3.1.1) are taken between each conductor, i, and the cell face. Each application of Faraday's law then gives a single row of a matrix equation. Similarly the integration surface in gauss' law (3.1.14) encloses each conductor, I of the n conductors in turn. Each application of Gauss' law then gives a row of a matrix equation. The resulting matrix system may be written as:

$$\frac{\partial(V)}{\partial z}+[R_0](I_z)+[L_0]\frac{\partial(I_z)}{\partial t}=E_{z\_tlm}[I] \qquad (3.2.1)$$

$$\frac{\partial(I_z)}{\partial z}+[G_0](V)+[C_0]\frac{\partial(V)}{\partial t}=(0) \qquad (3.2.2)$$

The TLM algorithm for solving such a system may also be generalized from the single to the multi-conductor case by the introduction of 'vector transmission lines' [4]. In such a vector transmission line the voltage and current states on the line are represented as vectors and the impedance becomes a matrix.

The multi-conductor TLM wire model interacts with the TLM field solution in the same manner as the single wire model by linking the wire model to the field model through an ideal transformer.

The embedded multi-conductor cable model is a circuit equivalent model and is therefore stable provided that all component values are positive. In the case of multi-conductor transmission line models we require that all the eigenvalues of the link and stub transmission line impedance matrices are positive. We therefore have a rigorous stability criterion for the model.

3.3 The TLM shielded cable model

The TLM shielded cable model is a development of the previously described embedded thin wire model [2,3,4]. The shielded cable model described here maintains the philosophy of developing the algorithm from an equivalent circuit of the cable propagation and includes the coupling of energy between the field and the cable in a self consistent manner. The shielded cable model presented here allows for coupling between the external illuminating field and the external shield. A transfer impedance term allows the coupling between the external shield current and the internal shielded mode. The transfer impedance includes an inductive and a resistive component.

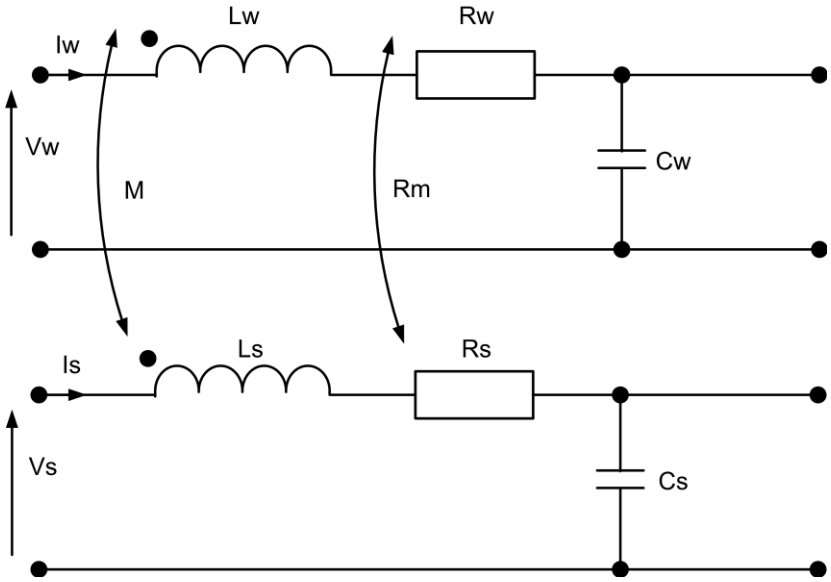

Figure 3.3.1. Shielded cable equivalent circuit.

The equivalent circuit for the shielded cable propagation is shown in figure 3.3.1. It should be noted that the voltages propagated in the shielded cable model are the shield voltage (Vs) and the inner conductor voltage with respect to the shield (Vw). The currents propagated are the external shield current (Is) and the inner conductor current (Iw). Since two different references are used for the cable voltages care should be exercised when applying conditions at cable terminations.

The two conductors are coupled through a mutual inductance, M, and a mutual resistance, Rm. Conductance terms are not included here. The propagation of signals on the two conductor system is described in the frequency domain by equations 3.3.1 and 3.3.2.

$$\frac{\partial}{\partial x}\begin{pmatrix} Vs(x) \\ Vw(x) \end{pmatrix} = \begin{bmatrix} j\omega Ls & j\omega M \\ j\omega M & j\omega Lw \end{bmatrix}\begin{pmatrix} Is(x) \\ Iw(x) \end{pmatrix} + \begin{bmatrix} Rs & Rm \\ Rm & Rw \end{bmatrix}\begin{pmatrix} Is(x) \\ Iw(x) \end{pmatrix} \qquad (3.3.1)$$

$$\frac{\partial}{\partial x}\begin{pmatrix} Is(x) \\ Iw(x) \end{pmatrix} = \begin{pmatrix} j\omega Cs & 0 \\ 0 & j\omega Cw \end{pmatrix}\begin{pmatrix} Vs(x) \\ Vw(x) \end{pmatrix} \qquad (3.3.2)$$

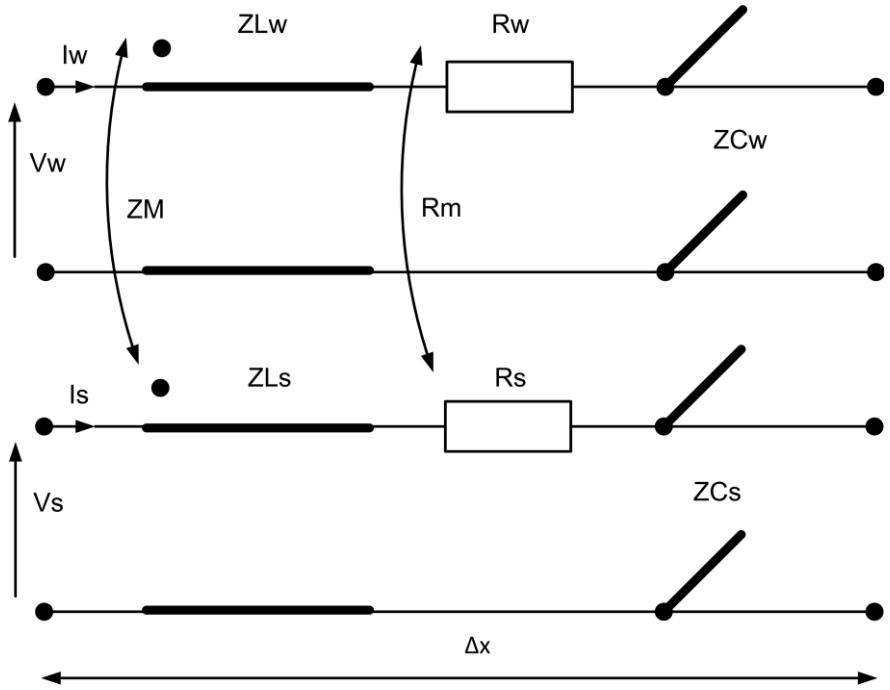

Figure 3.3.2. Shielded cable TLM model.

The voltages Vw and Vs may be written in terms of the voltages with respect to the TLM cell reference as

$$\begin{aligned} V_w &= V_w' - V_s' \\ V_s &= V_s' \end{aligned} \qquad (3.3.3)$$

Or in matrix form

$$\begin{pmatrix} V_w \\ V_s \end{pmatrix} = [T_v] \begin{pmatrix} V'_w \\ V'_s \end{pmatrix}, \quad [T_v] = \begin{bmatrix} 1 & -1 \\ 0 & 1 \end{bmatrix} \qquad (3.3.4)$$
$$(V_b) = [T_v](V_{b0})$$

Similarly the inner wire current and the outer shield current may be written in terms of the total conductor currents as

$$\begin{aligned} I_w &= I'_w \\ I_s &= I'_s + I'_w \end{aligned} \qquad (3.3.5)$$

Or in matrix form

$$\begin{pmatrix} I_w \\ I_s \end{pmatrix} = [T_I] \begin{pmatrix} I'_w \\ I'_s \end{pmatrix}, \quad [T_I] = \begin{bmatrix} 1 & 0 \\ 1 & 1 \end{bmatrix} \qquad (3.3.6)$$
$$(I_b) = [T_i](I_{b0})$$

Where the following notation has been introduced:

(ib) : branch current as propagated by the TLM cable model i.e. Iwire and Ishield

(ib0) : Total branch current i.e. Iwire and Iwire+Ishield

(vb) : branch voltage as propagated by the TLM cable model i.e. Vwire and Vshield

(vb0) : Total branch voltage i.e. Vwire+Vshield and Vshield

A TLM model of a short section, length Δx, of the shielded cable is shown in figure 3.3.2. The total inductance of the cable is embedded into the link lines and any additional capacitance required is incorporated into capacitive stub lines. The model of figure 3.3.2 is then embedded into a TLM field node in the manner described in section 3.1. Figure 3.3.3 shows the resulting equivalent circuit for a TLM node with an embedded cable traversing from left to right. In figure 3.3.3 the TLM model of the shielded cables on the left and right hand sides of the cell have been represented by Thevenin equivalent circuits derived from the transmission line topology of figure 3.3.2. The TLM field node is also represented by a Thevenin equivalent circuit. The coupling of energy between the field and the external shield conductor is included in the analysis through the ideal transformer. Note that there is no direct coupling of the external field to the inner conductor. The cables meet at the node centre where cables in the y and z directions may be electrically connected to internal connection nodes to form a junction.

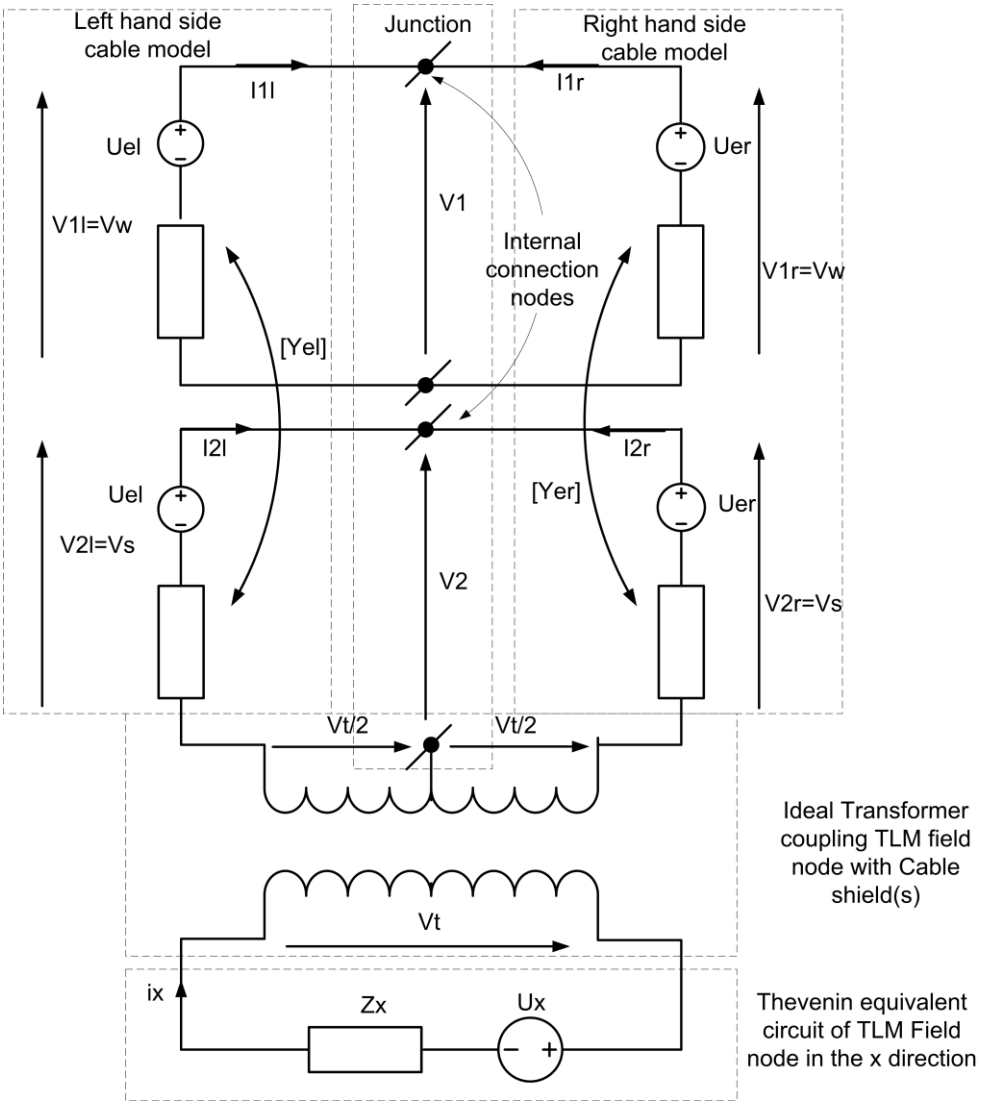

Figure 3.3.3. TLM node with embedded shielded cable model.

It should be noted that the Thevenin equivalent of the shielded cable includes terms which couple the shield to the inner wire through the admittance matrix. The circuit model in figure 3.3.3 describes the interaction of the shielded cable with the field and enables the scattering of voltage pulses in the cable model to be calculated as well as the effect of the cable on the field. This Thevenin equivalent may also incorporate the effect of voltage sources and loads on the individual conductors. The loads may be frequency dependent as described in section 6.

The following analysis is derived for the case of a cable traversing a cell from left to right through the TLM node. The analysis is general for an arbitrary number of shielded cables and includes junction conditions at the node centre.

The transformer voltage on the field side is given by:

$$V_t = U_x - Z_x i_x \qquad (3.3.7)$$

We introduce shielded cable column vectors on the left and right sides in which row i of Sc=1 if conductor i is not shielded and row I of Sc=0 otherwise. The field side transformer current is found from:

$$i_x = \frac{1}{2}\left(\left(Sc_l\right)^T\left(Ib_l\right) - \left(Sc_r\right)^T\left(Ib_r\right)\right) \qquad (3.3.8)$$

Where (Ib_l) and (Ib_r) are vectors of branch currents on the left and right hand sides of the node respectively. The voltage term contributed to each cable conductor on the left and right hand sides by the transformer are then:

$$\begin{aligned} Vg_l &= \left(Sc_l\right)\frac{v_t}{2} \\ &= \frac{U_x}{2}\left(Sc_l\right) + \frac{z_x}{4}\left(Sc_l\right)\left(\left(Sc_l\right)^T\left(Ib_l\right) - \left(Sc_r\right)^T\left(Ib_r\right)\right) \end{aligned} \qquad (3.3.9)$$

$$\begin{aligned} Vg_r &= \left(Sc_r\right)\frac{v_t}{2} \\ &= \frac{U_x}{2}\left(Sc_r\right) + \frac{z_x}{4}\left(Sc_r\right)\left(\left(Sc_l\right)^T\left(Ib_l\right) - \left(Sc_r\right)^T\left(Ib_r\right)\right) \end{aligned} \qquad (3.3.10)$$

(Vb_l) and (Vb_r) are introduced as branch voltage vectors on the left and right hand sides of the junction hence the conductor currents may be expressed as:

$$\left[Y_{el}\right]\left(\left(Ue_l\right) - \left(Vg_l\right) - \left(Vb_l\right)\right) = \left(Ib_l\right) \qquad (3.3.11)$$

$$\left[Y_{er}\right]\left(\left(Ue_r\right) + \left(Vg_r\right) - \left(Vb_r\right)\right) = \left(Ib_r\right) \qquad (3.3.12)$$

At the junction between the shielded cables Kirchhoff's current law is expressed (here assuming no coupling to cables in the y and z directions) as:

$$\left(In_l\right) + \left(In_r\right) = \left(0\right) \qquad (3.3.13)$$

where (In_l) and (In_r) are the vectors of total current incident on each of the internal connection nodes from the left and right respectively. (In_l) and (In_r) are expressed in terms of the total conductor currents, (ib0) using permutation matrices, [P]. The permutation matrices, [P], are defined as follows:

P(i,j) =1 if conductor j is connected to internal connection node i

P(i,j) =0 otherwise

Combining the permutation matrix, [P], with the current transformation matrix,[T_l] allows the cur rent incident on a node to be expressed in terms of the branch current as propagated by the TLM cable model:

$$\begin{aligned}(In_l) &= [P_l][T_{I,l}]^{-1}(Ib_l) = [PI_l](Ib_l)\\ (In_r) &= [P_r][T_{I,r}]^{-1}(Ib_r) = [PI_r](Ib_r)\end{aligned} \quad (3.3.14)$$

Similarly, the cable voltage vectors propagated in the TLM cable model for shielded cables (Vb) consist of voltages of shields with respect to the TLM node reference and voltages of the shielded conductors with respect to the shields.

The voltages on the internal connection nodes with respect to the reference conductors at the centre of the TLM cell are found in terms of the branch voltage as propagated by the TLM cable model as follows:

$$(Vn) = [P_l](Vb0_l) = [P_r](Vb0_r) \quad (3.3.15)$$

Expressing (Vb0) in terms of (Vb) gives

$$(Vn) = [P_l][Tv_l]^{-1}(Vb_l) = [P_r][Tv_l]^{-1}(Vb_r) \quad (3.3.16)$$

We also have:

$$(Vb0_l) = [P_l]^T(Vn), \quad (Vb0_r) = [P_r]^T(Vn) \quad (3.3.17)$$

Hence

$$(Vb_l) = [Tv_l][P_l]^T(Vn), \quad (Vb_r) = [Tv_r][P_r]^T(Vn) \quad (3.3.18)$$

Substituting equations 3.3.9 and 3.3.10 into 3.3.11 and 3.3.12 gives:

$$[Ye_l]\left((Ue_l) - \frac{U_x}{2}(Sc_l) - \frac{z_x}{4}(Sc_l)(Sc_l)^T(Ib_l) + \frac{z_x}{4}(Sc_l)(Sc_r)^T(Ib_r) - [Tv_l][Pv_l]^T(Vn)\right) = (Ib_l) \quad (3.3.19)$$

$$[Ye_l]\left((Ue_r) + \frac{U_x}{2}(Sc_r) - \frac{z_x}{4}(Sc_r)(Sc_l)^T(Ib_l) + \frac{z_x}{4}(Sc_r)(Sc_r)^T(Ib_r) - [Tv_r][Pv_r]^T(Vn)\right) = (Ib_r) \quad (3.3.20)$$

Combining equations 3.3.19 and 3.3.20 with 3.3.17 and rearranging leads to a system of equations of the form:

$$[Y](W) = [Y][Q](Vn) + [J](Ib) \quad (3.3.21)$$

Similarly equating the sum of the currents incident on the internal connection nodes from al drections, using equations 3.3.14 leads to:

$$[PI](Ib) = (0) \qquad (3.3.22)$$

where:

$$[Y] = \begin{bmatrix} [Ye_l] & [0] \\ [0] & [Ye_r] \end{bmatrix},$$

$$(W) = \begin{pmatrix} (Ue_l) - \frac{U^x}{2}(Sc_l) \\ (Ue_r) + \frac{U^x}{2}(Sc_r) \end{pmatrix}, (Ib) = \begin{pmatrix} (Ib_l) \\ (Ib_r) \end{pmatrix} \qquad (3.3.23)$$

$$[Q] = \begin{bmatrix} [Tv_l][Pv_l]^T \\ [Tv_r][Pv_r]^T \end{bmatrix}, \quad [J] = \begin{bmatrix} [Ye_l]\left[\frac{z^x}{4}(Sc_l)(Sc_l)^T\right] + [I] & -[Ye_l]\left[\frac{z^x}{4}(Sc_l)(Sc_r)^T\right] \\ -[Ye_r]\left[\frac{z^x}{4}(Sc_r)(Sc_l)^T\right] & [Ye_r]\left[\frac{z^x}{4}(Sc_r)(Sc_r)^T\right] + [I] \end{bmatrix} \qquad (3.3.24)$$

Hence:

$$(Ib) = [J]^{-1}[Y][Q](Vn) - [J]^{-1}[Y](W) \qquad (3.3.25)$$

Equation 3.3.22 gives

$$[PI](Ib) = [PI][J]^{-1}[Y][Q](Vn) - [PI][J]^{-1}[Y](W) = (0) \qquad (3.3.26)$$

We can now solve for the internal connection node voltages as:

$$(Vn) = \left[[PI][J]^{-1}[Y][Q]\right]^{-1}[PI][J]^{-1}[Y](W) \qquad (3.3.27)$$

Equation 3.3.17 then gives the branch voltages and the branch currents are then found from equations 3.3.11 and 3.3.12. Knowledge of the branch voltages enables the scattered voltage pulses on the shielded cable to be calculated.

The total current in the field side of the node is found from 3.3.8 and hence the voltages scattered from the TLM field node may be corrected to take account of the cable current.

The connection process in which the cable voltages are updated at the half time step at faces between TLM cells proceeds in a similar manner to the cell centre update but in the absence of the

field to cable coupling i.e. the TLM field node circuit and the ideal transformer are removed. This can be achieved in the above analysis by setting the shielded cable vectors (Sc_l) and (Sc_r) to zero in the above analysis. This leaves open the opportunity to apply junction conditions between cables at TLM cell faces, although this is not done within **GGI_TLM**.

Boundary conditions may be applied at cell faces such as short circuit conditions to represent connection of a cable conductor to a PEC surface. Lumped loads and sources may be also be readily included in the model.

4 Cable junctions

The connectivity of conductors at junctions can be complex. In addition a 'V=0' boundary condition may be applied to indicate connection of conductors to a surface in the mesh. The connectivity of conductors is described by first setting up a number of internal connection nodes at the junction. A permutation matrix (P) then describes how individual conductors within a cable are connected to the internal connection nodes.

The number of rows in the permutation matrix is equal to the number of internal connection nodes, the total number of columns is the total number of conductors incident on the junction. Permutation matrices may therefore be quite large if a number of cables are connected at a junction. In order to simplify the specification of P matrices they are defined on a cable by cable basis and the full permutation matrix for a junction is built within **GGI_TLM**. The elements of a P matrix defined on a cable by cable basis are defined as:

P_{ij}=1 if conductor j connects to internal connection node i

P_{ij}=0therwise

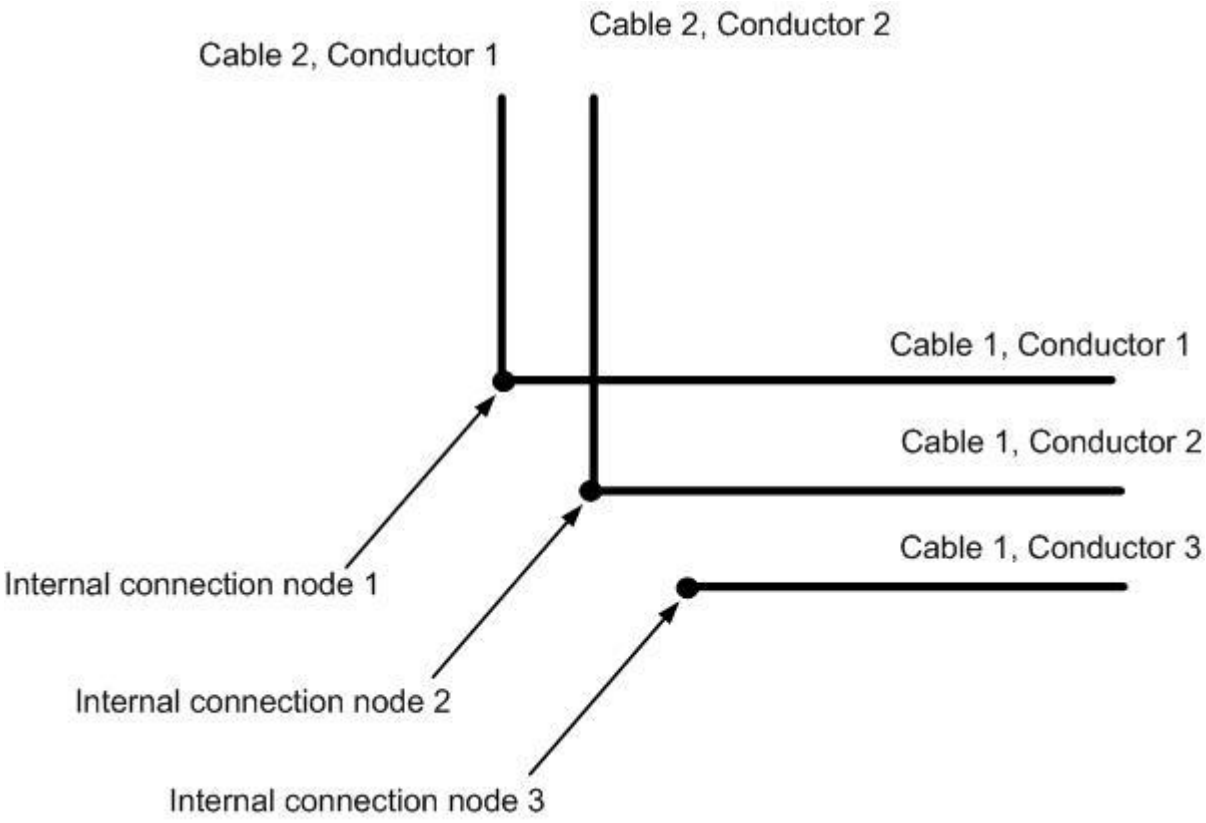

Figure 4.1.1. Normal junction

For the junction in figure 4.1.1 above there are two P matrices one for each of the two cables.

$$PI_1 = \begin{bmatrix} 1 & 0 & 0 \\ 0 & 1 & 0 \\ 0 & 0 & 1 \end{bmatrix}$$
$$PI_2 = \begin{bmatrix} 1 & 0 \\ 0 & 1 \\ 0 & 0 \end{bmatrix} \qquad (4.1.1)$$

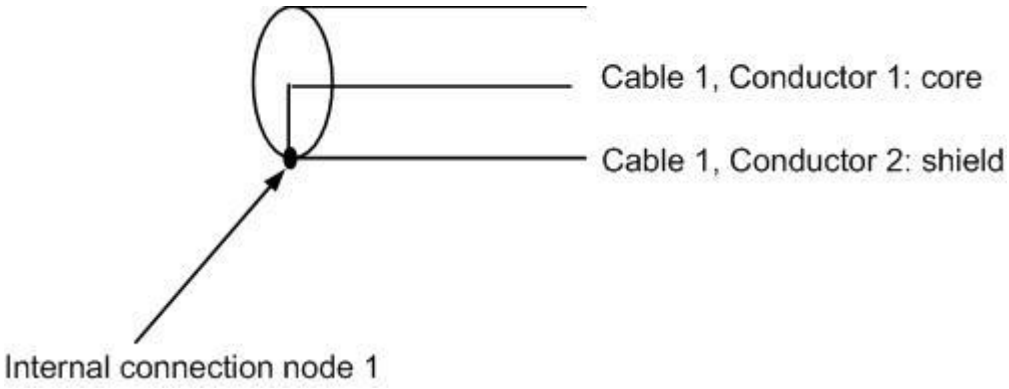

Figure 4.1.2. Coaxial cable termination.

In figure 4.1.2 a coaxial cable is terminated by a short circuit. For this case there is a single P matrix

$$PI = [1 \quad 1] \qquad (4.1.2)$$

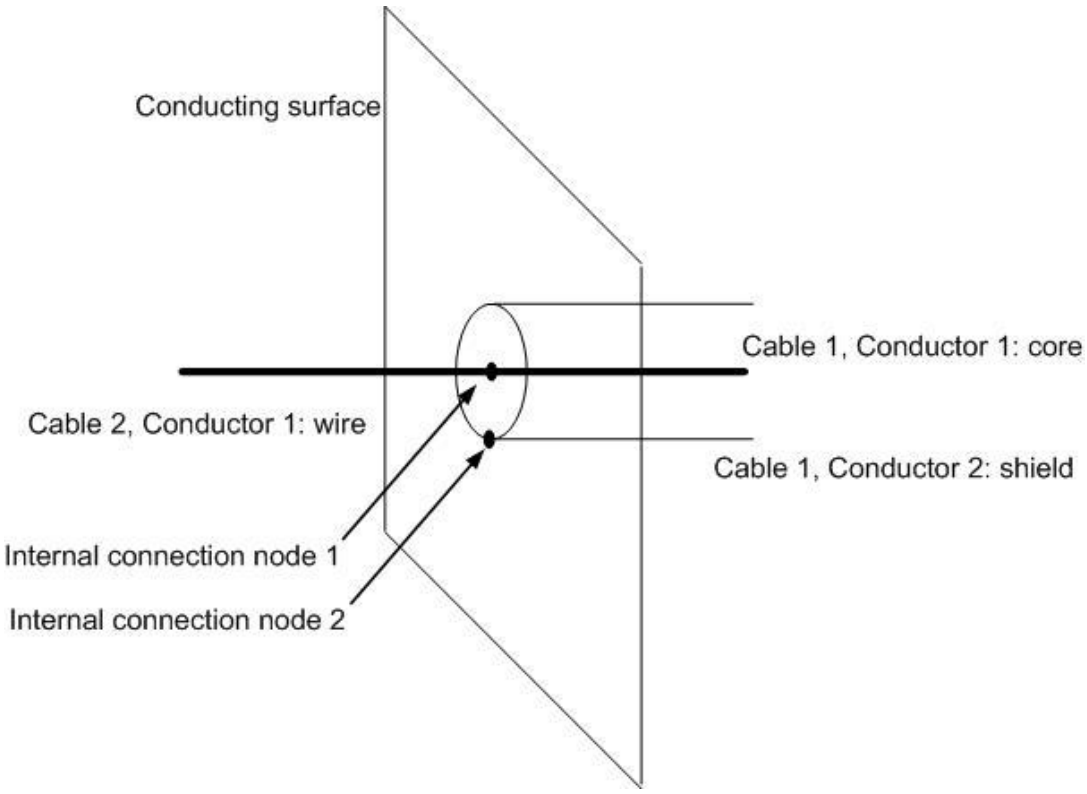

Figure 4.1.3. Coax to monopole transition

The P matrices to specify the coax to monopole transition in figure 4.1.3 are as follows

$$PI_1 = \begin{bmatrix} 1 & 0 \\ 0 & 1 \end{bmatrix}$$
$$PI_2 = \begin{bmatrix} 1 \\ 0 \end{bmatrix} \qquad (4.1.3)$$

In this case a termination rather than a junction is required since we are connecting to a surface. A boundary condition must also be set on internal connection node 2 as described in the termination_list packet data.

5 TLM cable termination model

It has been described in previous sections how boundary and termination conditions may be incorporated into the cable model connection process. In this section we develop and present the solution for a general cable termination in which individual conductors may be grounded to a conducting surface with our without loads and sources, terminated in free space or connected to conductors in an adjacent cell. A typical situation is shown in figure 5.1 in which there are cables

incident from left and right. Each cable has a load and a voltage source associated with it, there are open circuit, short circuit and straight through connections. The analysis of the termination is similar to that of the cell centre junction in the absence of the field coupling term. A significant difference is the possibility of a short circuit termination and the presence of a voltage source and load impedance on the conductors.

As at the cell centre internal connection nodes are defined and the topology of the connection is described by the use of permutation matrices which are defined on the left and right hand sides of the termination. We define voltage transformation matrices, [Tv], and permutation matrices, [P], for the termination in the same way as for a junction (section 3.3)

P(i,j) =1 if conductor j is connected to internal connection node i

P(i,j) =0 otherwise.

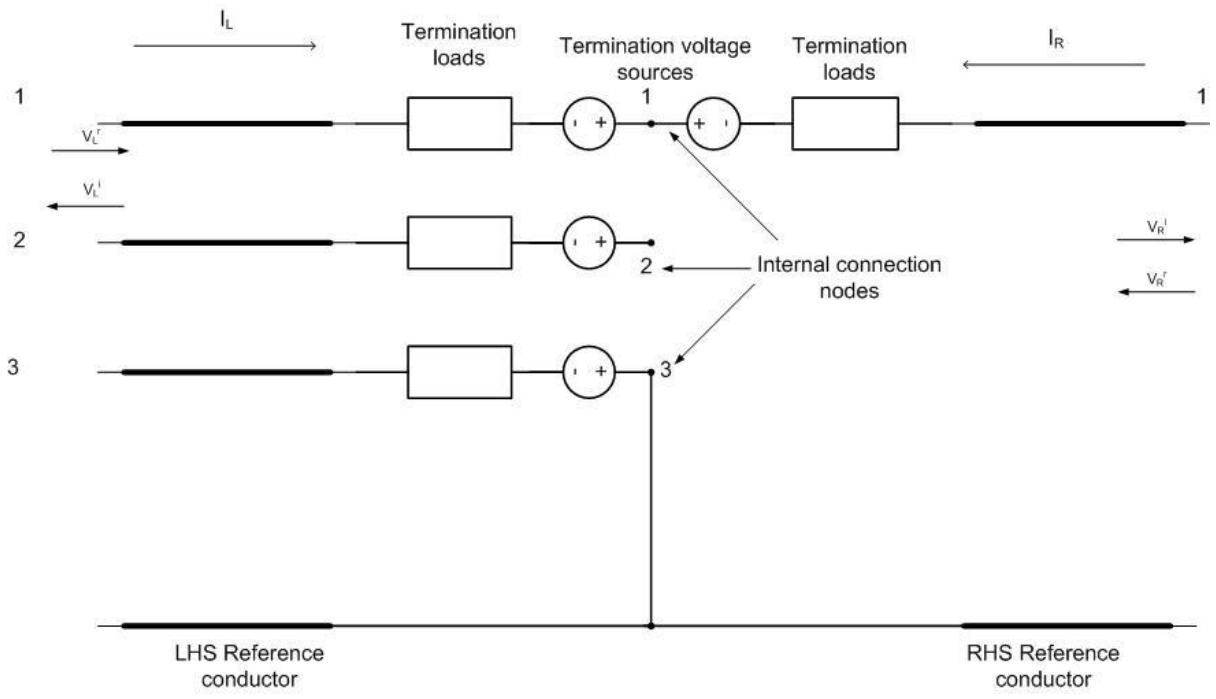

Figure 5.1. Multi-conductor termination.

A boundary condition matrix, [S], is defined of dimension n_int×n_ext. The elements of the rows of the matrix are zero unless the corresponding internal connection node is connected to ground in which case the whole row takes the value 1. The revised permutation matrix is then defined by

$$[P'] = [P] - [S] \qquad (5.1.1)$$

In the case of the example above we have

$$[PI_L]=\begin{bmatrix}1&0&0\\0&1&0\\0&0&1\end{bmatrix},\quad [S_L]=\begin{bmatrix}0&0&0\\0&0&0\\1&1&1\end{bmatrix},\quad [PI_L]'=\begin{bmatrix}1&0&0\\0&1&0\\-1&-1&0\end{bmatrix}$$
$$[PI_R]=\begin{bmatrix}1\\0\\0\end{bmatrix},\quad [S_R]=\begin{bmatrix}0\\0\\1\end{bmatrix},\quad [PI_R]'=\begin{bmatrix}1\\0\\-1\end{bmatrix} \qquad (5.1.2)$$

The individual conductor voltages on the left and right hand sides are found from the voltages at the internal connection nodes, (Vn), as

$$(Vb_l)=[Tv_l][P_l]^T(Vn),\quad (Vb0_r)=[Tv_r][P_r]^T(Vn) \qquad (5.1.3)$$

Where here we use the original [P] matrices.

Kirchoff's current law is then expressed as

$$[P_L]'(Ib_L)+[P_R]'(Ib_R)=(0) \qquad (5.1.4)$$

A Thevenin equivalent of the combined transmission lines, sources and loads is formed on the left and right hand sides with vector voltage sources (U_{el}) and (U_{er}) and with admittance matrices [Y_{el}] and [Y_{er}].

The individual conductor currents are expressed in terms of the Thevenin equivalent circuit components

$$[Y_{eL}]((U_{eL})-(Vb_L))=(Ib_L) \qquad (5.1.5)$$

$$[Y_{eR}]((U_{eR})-(Vb_R))=(Ib_R) \qquad (5.1.6)$$

The conductor voltages are written in terms of the internal connection node voltages thus

$$[Y_{el}]((Ue_L)-)[Tv_l][Pv_l]^T(Vn)=(Ib_L) \qquad (5.1.7)$$

$$[Y_{eR}]\left((U_{eR})-[Tv_r][Pv_r]^T(Vn)\right)=(Ib_R) \qquad (5.1.8)$$

Substituting the expressions for the conductor currents into equation 5.1.3 gives

$$[PI_L]'[Y_{eL}]\left((Ue_L)-[Tv_l][Pv_l]^T(Vn)\right)+[PI_R]'[Y_{eR}]\left((Ue_R)-[Tv_r][Pv_r]^T(Vn)\right)=(0) \qquad (5.1.9)$$

$$\left[[PI_L]'[Y_{eL}][Tv_l][Pv_l]^T+[P_R]'[Y_{eR}][Tv_r][Pv_r]^T\right](Vn)=\left([PI_L]'[Y_{eL}](Ue_L)+[PI_R]'[Y_{eR}](Ue_R)\right) \qquad (5.1.10)$$

If a boundary condition V=0 is applied to one of the internal connection nodes then the equation for this voltage is found to be a linear combination of the other equations. The corresponding row and column of the system are removed before expressing the solution for the unknown internal connection node voltages as

$$(Vn)=\left[[P_L]'[Y_{eL}][Tv_l][P_l]^T+[P_R]'[Y_{eR}][Tv_r][P_r]^T\right]^{-1}\left([P_L]'[Y_{eL}](Ue_L)+[P_R]'[Y_{eR}](Ue_R)\right)$$

(5.1.11)

The conductor voltages and currents are given by equation 5.1.3. The voltage pulses scattered into the wire model vector link lines may then be calculated in a similar manner to the junction (section 3.3).

6 Frequency dependent termination impedance model

6.1 Digital filter implementation

Suppose we have a termination impedance with the frequency response given by a rational function in complex frequency:

$$Z(j\omega)=\frac{a_0+a_1(j\omega)+a_2(j\omega)^2+\ldots}{b_0+b_1(j\omega)+b_2(j\omega)^2+..} \qquad (6.1.1)$$

The frequency dependent impedance properties are implemented in TLM as a digital filter. The filter coefficients are obtained by application of the bilinear transformation.

$$j\omega\rightarrow\frac{2}{\Delta t}\left(\frac{1-z^{-1}}{1+z^{-1}}\right) \qquad (6.1.2)$$

Note: The bilinear transformation is not the only transformation which will give valid filter coefficients, it does have the advantage of always providing a stable digital filter from a stable transfer function.

This results in a rational function in z^{-1} where z^{-1} is the time shift operator, corresponding to a shift of 1 time step. Following the bilinear transformation we have

$$Z(z^{-1})=\frac{V(z^{-1})}{I(z^{-1})}=\frac{a_0'+a_1'z^{-1}+a_2'z^{-2}+\ldots}{b_0'+b_1'z^{-1}+b_2'z^{-2}+\ldots} \qquad (6.1.3)$$

This implies that

$$b_0'V^n+b_1'V^{n-1}+b_2'V^{n-2}+\ldots=a_0'I^n+a_1'I^{n-1}+a_2'I^{n-2}+\ldots \qquad (6.1.4)$$

which we can rearrange to calculate V from I (or I from V) at time step n in terms of V at the current time step and both V and I at previous time steps e.g.

$$V^n = \frac{1}{b_0'}\left(a_0' I^n + a_1' I^{n-1} + a_2' I^{n-2} + \ldots - \left(b_1' V^{n-1} + b_2' V^{n-2} + \ldots\right)\right) \qquad (6.1.5)$$

The above form is not the most efficient implementation in terms of the required memory as we will need to store (2×model order) real numbers. A more efficient implementation is found as follows:

$$V(z^{-1}) = I(z^{-1})Z(z^{-1}) = I(z^{-1})\frac{A(z^{-1})}{B(z^{-1})} \qquad (6.1.6)$$

We introduce W as

$$V(z^{-1}) = W(z^{-1})A(z^{-1}), \quad W(z^{-1}) = \frac{I(z^{-1})}{B(z^{-1})} \qquad (6.1.7)$$

This leads to the two stage update

$$W^n = \frac{1}{b_0'}\left(I^n - \left(b_1' W^{n-1} + b_2' W^{n-2} + \ldots\right)\right) \qquad (6.1.8)$$

$$V^n = \left(a_0' W^n + a_1' W^{n-1} + a_2' W^{n-2} + \ldots\right) \qquad (6.1.9)$$

Where we only need to store (1×model order) real numbers

This implementation may be represented in a circuit form

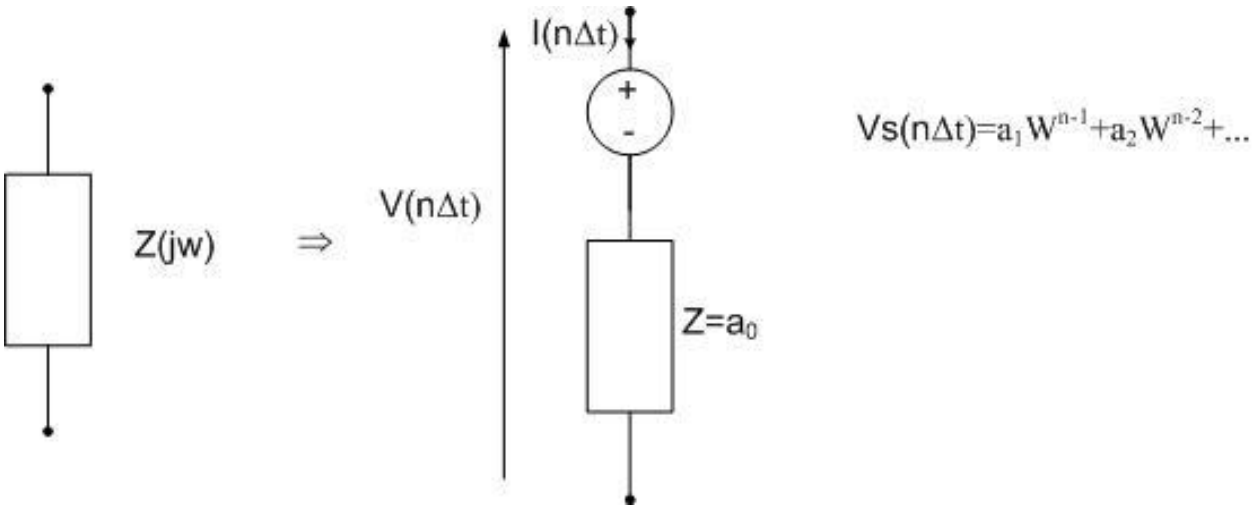

Figure 6.1.1.

6.2 Example1.

If we wish to model an inductor with impedance

$$Z(jw) = j\omega L \qquad (6.2.1)$$

Application of the bilinear transform gives:

$$Z(z^{-1}) = \frac{V(z^{-1})}{I(z^{-1})} = \left(\frac{\frac{2}{\Delta t} - \frac{2}{\Delta t} z^{-1}}{1 + z^{-1}} \right) L \qquad (6.2.2)$$

Using the implementation described above:

$$Z(z^{-1}) = \frac{2L}{\Delta t} - \frac{\frac{4L}{\Delta t} z^{-1}}{1 + z^{-1}} \qquad (6.2.3)$$

$$V^n = \left(\frac{2L}{\Delta t} I^n \quad - \frac{4L}{\Delta t} W_1^{n-1} \right) \qquad (6.2.4)$$

$$W_1^n = I^n - W_1^{n-1} \qquad (6.2.5)$$

If we define: $Z_L = \frac{2L}{\Delta t}$ and $V_r^n = Z_L W_1^n$ then the update can be expressed as

$$V^n = \left(Z_L I^n \quad - 2V_r^{n-1} \right) \qquad (6.2.6)$$

$$V_r^n = Z_L I^n - V_r^{n-1} \qquad (6.2.7)$$

Introducing the variable $V_i^n = -V_r^{n-1}$ then enables us to recover the traditional TLM model of an inductor through the update process:

1. Calculate the voltage across the Thevenin equivalent circuit

$$V^n = \left(Z_L I^n \quad + 2V_i^n \right) \qquad (6.2.8)$$

2. Calculate the voltage reflected back into the stub transmission line

$$V_r^n = Z_L I^n + V_i^n \qquad (6.2.9)$$

3. Reflection of the transmission line voltage with reflection coefficient -1 which becomes the incident voltage at the next timestep

$$V_i^{n+1} = -V_r^n \qquad (6.2.10)$$

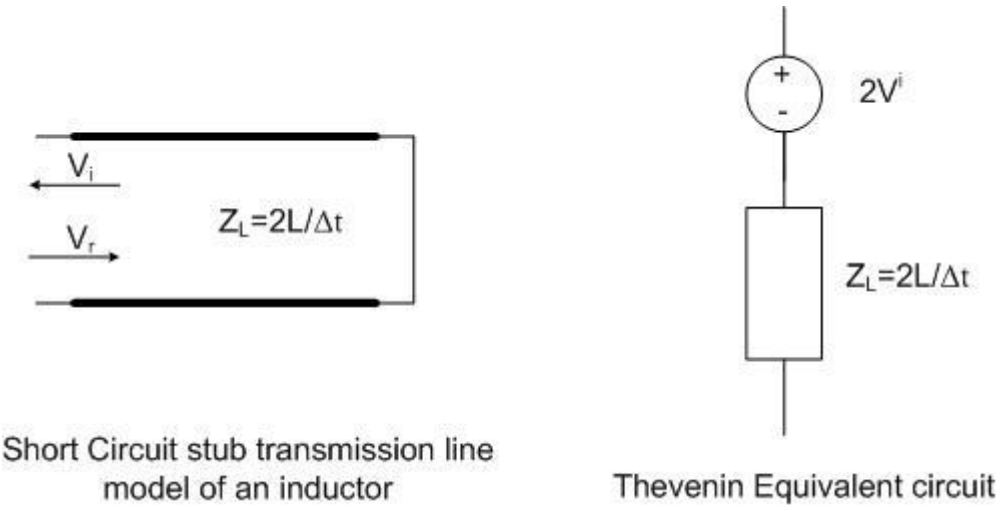

Figure 6.2.1.

6.3 Example2.

If we wish to model a capacitor with impedance

$$Z(jw) = \frac{1}{j\omega C} \qquad (6.2.11)$$

Application of the bilinear transform gives:

$$Z(z^{-1}) = \frac{V(z^{-1})}{I(z^{-1})} = \left(\frac{1+z^{-1}}{\frac{2C}{\Delta t} - \frac{2C}{\Delta t} z^{-1}} \right) \qquad (6.2.12)$$

Using the implementation described above:

$$Z(z^{-1}) = \frac{\Delta t}{2C} + \frac{2z^{-1}}{\frac{2C}{\Delta t} - \frac{2C}{\Delta t} z^{-1}} = \frac{\Delta t}{2C} + \frac{2\frac{\Delta t}{2C} z^{-1}}{1 - z^{-1}} \qquad (6.2.13)$$

$$V^n = \left(\frac{\Delta t}{2C} I^n \quad + 2\frac{\Delta t}{2C} W_1^{n-1} \right) \qquad (6.2.14)$$

$$W_1^n = I^n + W_1^{n-1} \qquad (6.2.15)$$

If we define: $Z_c = \frac{\Delta t}{2C}$ and $V_r^n = Z_C W_1^n$ then the update can be expressed as

$$V^n = \left(Z_C I^n \quad + 2V_r^{n-1} \right) \qquad (6.2.16)$$

$$V_r^n = Z_C I^n + V_r^{n-1} \qquad (6.2.17)$$

Introducing the variable $V_i^n = V_r^{n-1}$ then enables us to recover the traditional TLM model of a capacitor through the update process:

4. Calculate the voltage across the Thevenin equivalent circuit

$$V^n = \left(Z_C I^n \quad + 2V_i^n \right) \qquad (6.2.18)$$

5. Calculate the voltage reflected back into the stub transmission line

$$V_r^n = Z_C I^n + V_i^n \qquad (6.2.19)$$

6. Reflection of the transmission line voltage with reflection coefficient +1 which becomes the incident voltage at the next timestep

$$V_i^{n+1} = V_r^n \qquad (6.2.20)$$

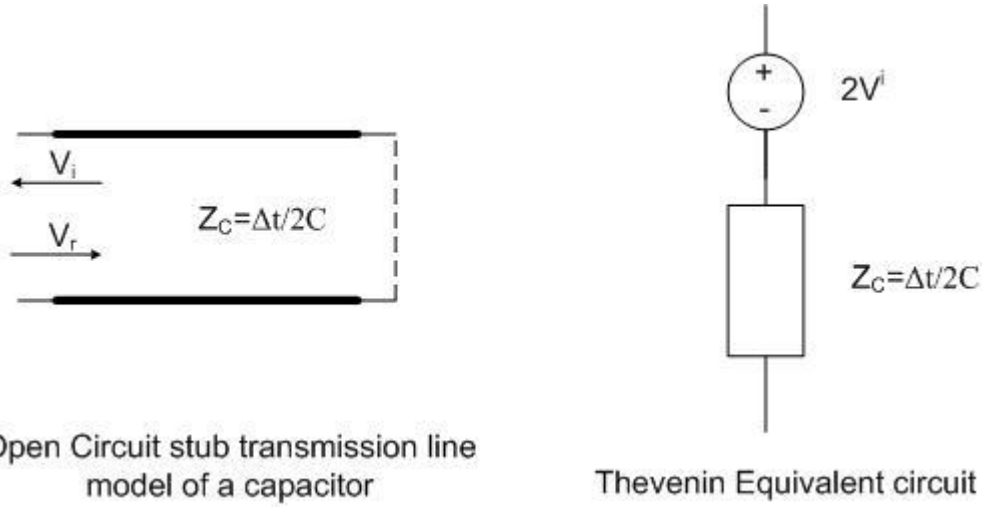

Figure 6.3.1

7 Cable modeling process

Cell centre scattering process t=nΔt:

1. Get the cell centre Thevenin equivalent circuit parameters (Z, V) for the given field update scheme
2. Calculate source voltages and update any filters used to implement frequency dependent loads.
3. Solve the cell centre field/ wire circuit for the wire current and voltage
4. Calculate voltage pulses scattered into wire model link and stub lines from the cell centre
5. Update the field scattering/ field update due to the presence of the wire (current flowing at the cell centre)

Cell face connection process t=(n+½)Δt:

1. Calculate source voltages and update any filters used to implement frequency dependent loads.
2. Solve the cell face circuit for the wire current and voltage
3. Scatter the appropriate voltage pulses back into the wire link lines

8 References

[1] Paul, C, "Analysis of multi-conductor transmission lines," 2nd edition, Wiley, 2007

[2] Paul, J.; Christopoulos, C.; Thomas, D.W.P.; Xilei Liu. "Time-domain modeling of electromagnetic wave interaction with thin-wires using TLM," IEEE Trans. EMC, Volume 47, Aug. 2005, pp 447-455.

[3] Paul, J.; Christopoulos, C.; Thomas, D. W. P. "Correction to "Time-Domain Modeling of Electromagnetic Wave Interaction With Thin-Wires Using TLM" [Aug 05 447-455]. IEEE Trans. EMC, Volume 50, May 2008, pp 450-451.

[4] Wlodarczyk, A.J.; Trenkic, V.; Scaramuzza, R.A.; Christopoulos, C. "A fully integrated multiconductor model for TLM," IEEE Trans. MTT, Volume 46, No 2, Dec 1998, pp 2431-2437.